Acute death of astrocytes in blast-exposed rat organotypic hippocampal slice cultures

Anna P. Miller[1,2,3], **Alok S. Shah**[1,3], **Brandy V. Aperi**[1,3], **Shekar N. Kurpad**[1,2,3], **Brian D. Stemper**[1,3], **Aleksandra Glavaski-Joksimovic**[1,2,3]*

1 Department of Neurosurgery, Medical College of Wisconsin, Milwaukee, Wisconsin, United States of America, **2** Department of Cell Biology, Neurobiology & Anatomy, Medical College of Wisconsin, Milwaukee, Wisconsin, United States of America, **3** Clement J. Zablocki Veterans Affairs Medical Center, Milwaukee, Wisconsin, United States of America

* aglavaski@mcw.edu

Abstract

Blast traumatic brain injury (bTBI) affects civilians, soldiers, and veterans worldwide and presents significant health concerns. The mechanisms of neurodegeneration following bTBI remain elusive and current therapies are largely ineffective. It is important to better characterize blast-evoked cellular changes and underlying mechanisms in order to develop more effective therapies. In the present study, our group utilized rat organotypic hippocampal slice cultures (OHCs) as an *in vitro* system to model bTBI. OHCs were exposed to either 138 ± 22 kPa (low) or 273 ± 23 kPa (high) overpressures using an open-ended helium-driven shock tube, or were assigned to sham control group. At 2 hours (h) following injury, we have characterized the astrocytic response to a blast overpressure. Immunostaining against the astrocytic marker glial fibrillary acidic protein (GFAP) revealed acute shearing and morphological changes in astrocytes, including clasmatodendrosis. Moreover, overlap of GFAP immunostaining and propidium iodide (PI) indicated astrocytic death. Quantification of the number of dead astrocytes per counting area in the hippocampal cornu Ammonis 1 region (CA1), demonstrated a significant increase in dead astrocytes in the low- and high-blast, compared to sham control OHCs. However only a small number of GFAP-expressing astrocytes were co-labeled with the apoptotic marker Annexin V, suggesting necrosis as the primary type of cell death in the acute phase following blast exposure. Moreover, western blot analyses revealed calpain mediated breakdown of GFAP. The dextran exclusion additionally indicated membrane disruption as a potential mechanism of acute astrocytic death. Furthermore, although blast exposure did not evoke significant changes in glutamate transporter 1 (GLT-1) expression, loss of GLT-1-expressing astrocytes suggests dysregulation of glutamate uptake following injury. Our data illustrate the profound effect of blast overpressure on astrocytes in OHCs at 2 h following injury and suggest increased calpain activity and membrane disruption as potential underlying mechanisms.

Introduction

The rate of blast-induced traumatic brain injury (bTBI) has escalated among active duty military personnel and veterans involved in recent military campaigns [1–4]. Symptoms of bTBI manifest on a scale of mild to severe and often involve physical, cognitive, emotional, and social deficits [5–10]. Moreover, a soldier's reluctance to seek treatment [11], compounded with a potential misdiagnosis of post-traumatic stress disorder (PTSD) [3, 5] can impede recovery. Current treatment strategies are mainly focused on rehabilitation, mental health services, and symptom amelioration [12]. However, there is no available therapy that can stop or reverse the neurodegenerative cascade that follows primary cell death caused by blast exposure. Moreover, mechanisms underlying early and delayed cell death following bTBI remain elusive. Preclinical and clinical data suggest different underlying mechanisms and injury manifestations between blunt TBI and bTBI [13–16]. For these reasons, answering fundamental questions regarding bTBI neuropathology is prerequisite for the development of more effective therapy protocols. Specifically, it is necessary to assess early cellular and molecular changes following bTBI to establish potential therapeutic strategies to prevent or ameliorate the spread of neurodegeneration.

Direct effects of blast exposure on brain tissue remain controversial. It has been proposed that blast overpressure indirectly causes brain injury either via skull deformation, head acceleration, ischemia, or thoracic mechanisms [17–23]. However, research from our group, in addition to the results of other experts in the field, suggests that a blast shock wave can transverse the cranium intact and generate tissue stress and strain leading to neuronal damage [24–29]. Correspondingly, data from *in vitro* bTBI models [30–33], including our recent findings [34], imply that blast overpressure can directly damage neurons and glial cells. In previous rat bTBI studies conducted by our [16, 28] and other groups [19, 35, 36], exposure to the peak overpressure magnitudes in the range of 100 to 450 kPa resulted in neurodegenerative changes and behavioral impairments. Likewise, exposure of OHCs to the blast overpressures of about 150 (low) and 280 kPa (high) in our previous [34] and present *in vitro* studies evoked significant and progressive cell death, confirming validity of our test conditions.

Neurodegenerative disorders are traditionally investigated with a neuron-centric approach, but it is becoming increasingly recognized that glial cells, including astrocytes, are implicated in neurodegenerative disorders and brain injury [37–41]. Under normal physiological conditions, astrocytes play a pivotal role in maintenance of brain homeostasis through control over cerebral blood flow and metabolism, ionic spatial buffering, regulation of water, control of biosynthesis and turnover of amino acid neurotransmitters, and providing energy and nutrient support for neurons [42–47]. Astrocytes also have the ability to control synaptogenesis, integrate neuronal inputs, release a variety of transmitters, and modulate synaptic activity [48–54]. However, astrocytes are affected in many neurodegenerative disorders [55–59], and their altered function contributes to further spread of neurodegenerative changes [60–62]. Although the exact role of astrocytes in neurodegeneration is unknown, it is believed that different mechanisms such as change in glutamate uptake and release, activation of astrocytes, and their death may contribute to neuronal loss [37, 38, 58, 63, 64]. Changes in astrocytic functions and the above mechanisms have also been associated with TBI [40, 41, 65]. Though largely dependent on severity and mechanical properties of the injury, reactive astrogliosis has been observed following both blunt and bTBI [35, 40, 66–69]. Spectrum of morphological, molecular and functional changes that astrocytes undergo in reactive astrogliosis, also known as astrocytosis, include upregulation of glial fibrillary acidic protein (GFAP) and other intermediate filaments, hypertrophy of cell body and processes, and in more severe cases proliferation and scar formation [70]. Additionally, several animal [71–75] and human [76] non-blast TBI

studies have indicated death of astrocytes by the decrease in the total number of cells labeled with the astrocytic marker GFAP, or by co-staining with GFAP and markers of apoptotic cell death including terminal deoxynucleotidyl transferase dUTP nick end labeling (TUNEL) and activated caspase 3. In human postmortem material obtained from cases with severe and complicated TBI, astrocytes that underwent an continuum of oncosis, apoptosis and necrosis were detected based on morphological changes such as swollen nucleoplasm, cytoplasm, and cell organelles, chromatin condensation and marginalization, formation of apoptotic bodies, and plasma membrane fragmentation [77]. Two recent studies also reported presence of dead, TUNEL and GFAP co-labeled astrocytes in rat and monkey bTBI models [67, 78]. However, the exact role of astrocytic activation and death in the etiology of bTBI is unclear and the acute response of astrocytes to a blast overpressure is not well characterized. Therefore, our present study focuses on understanding how astrocyte morphology and viability are affected by a blast overpressure at an early time point following injury and to elucidate mechanisms underlying blast-evoked astrocytic death.

Our previous studies in *in vitro* bTBI model were mainly focused on characterizing the neuronal and glial response to blast exposure at 72 hours (h) post-injury [34]. At this time point, we demonstrated significant neuronal loss and robust activation of astrocytes and microglial cells in OHCs exposed to blast overpressure [34]. While only a small number of dead glial cells were present at 72 h post-injury, dead microglial cells were observed at 4 and 24 h post injury [34]. The aim of the current study was to characterize the acute astrocytic response to a blast overpressure exposure using the same *in vitro* bTBI model. As done previously in studies utilizing OHCs [79–81], we have visualized astrocytes using immunostaning against GFAP that is expressed in the large portion of heterogeneous population of astrocytes [70, 82]. Additionally, co-labeling of GFAP with propidium iodide (PI) or Annexin V was used to assess necrotic or apoptotic astrocytic death, respectively. To further study mechanisms that lead to the early blast-evoked astrocytic death, immunohistochemical staining, western blot, and a dextran permeability assay were conducted. Contrary to our previous data collected in *in vitro* bTBI model at 72 h post-injury, present study demonstrated significant number of dead, necrotic astrocytes at 2 h post-injury, suggesting different response of astrocytes at the acute and the later phase of bTBI. An understanding of different temporal effects of blast exposure on astrocytes is of the particular interest in illuminating mechanisms that lead to the spread of neurodegeneration and development of more effective therapies for bTBI.

Methods

Animals

Time-pregnant, Sprague Dawley (SD) rats (Charles River Laboratories, Wilmington, MA, USA) were housed in individual cages, with standard colony conditions, until parturition. Food and water were available *ad libitum*. Hippocampal tissue used to prepare OHCs was obtained from postnatal rats (P7-P10; n = 59). All laboratory animal procedures were completed in congruence with the National Institutes of Health (NIH) Guide for the Care and Use of Laboratory Animals and approved by the Zablocki Veterans Affairs Subcommittee for Animal Studies (Protocol number: 3171–01).

Preparation of OHCs

OHCs were prepared under aseptic conditions using a modified procedure from Stoppini and colleagues [34, 83]. Postnatal rats were euthanized via decapitation and the brains were removed via a longitudinal cut along the midline of the skull. The hippocampi were isolated in cold dissecting medium (pH 7.2) which was composed of 50% Minimum Essential Medium

(MEM), 50% calcium and magnesium free Hanks Balanced Salt Solution (HBSS), 20 mM HEPES (N-2- hydroxyethylpiperazine-N'-2-ethanesulfonic acid), 7.5 g/l D-glucose, and 1% Penicillin/Streptomycin (all obtained from ThermoFisher Scientific, Grand Island, NY, USA) [34, 84]. Using a McIlwain tissue chopper (Ted Pella, Inc., Redding, CA, USA) hippocampi were cut transversely into 400 μm-thick sections. Hippocampal sections were separated under a dissecting microscope with sterile spatulas and inspected for intact morphology. Only intact sections were transferred to 0.4 μm porous MilliCell cell culture inserts (EMD Millipore, Billerica, MA, USA) and grown in 6-well plates containing 1 ml of serum-based media consisting of 50% MEM- Hanks medium, 25% HBSS, 25% horse serum, 50 mM HEPES, 2 mM L-glutamine, 5 mg/ml D glucose, and 1% antibiotic/antimycotic (all obtained from ThermoFisher Scientific except horse serum which was obtained from Atlanta Biologicals, Flowery Branch, GA, USA) [34, 85–87]. OHCs were maintained at 37°C with 5% CO_2 for the duration of the studies.

One day following dissection, the culture media was replaced with fresh serum-based media. From 4 to 7 days *in vitro* (DIV), the serum-based media was gradually changed to serum-free media consisting of 50% MEM- Hanks, 25% HBSS, 25% Neurobasal-A medium, 17 mM HEPES, 2 mM L-Glutamine, 2% B-27, 5 mg/ml D-glucose, and 1% antibiotic/antimycotic (all obtained from ThermoFisher Scientific). Starting from the 7th DIV until the end of experiment, OHCs were maintained in the serum-free media [34, 86, 88] in order to decrease glial activation, proliferation and scar formation [79, 89]. As described below, PI uptake measurements were also performed in serum-free media as DNase I present in the serum can degrade the DNA of dead cells and lead to an inaccurate estimate of the number of dead cells [90].

Blast injury of OHCs with an open-ended helium-driven shock tube

OHCs were grown for 8 days in culture prior to blast exposure. As previously demonstrated by data from our and other laboratories, this period is sufficient to allow recovery from any procedure-related degeneration [34, 91, 92]. An open-ended, helium-driven shock tube, built by our group, was used to generate overpressures of specific magnitudes and to produce injury in OHCs as described previously [34]. Briefly, individual membrane inserts containing OHCs were placed in 40-mm culture dishes with 800 μl of serum-free media. Culture dishes were next covered with Parafilm and sealed within sterile plastic pouches (5.5 cm x 6.5 cm). OHCs were placed on a rigid stand 22 cm away from the end of the shock tube and were positioned 55° off axis to avoid exposure to exhaust gases. OHCs were injured using a single blast overpressure designated as either low (138 ± 22 kPa) or high (273 ± 23 kPa), since our previous studies demonstrated that exposure to overpressures of about 150 kPa and 280 kPa results in significant cell death at 2 h following injury [34]. Sham control OHCs were processed identical to blast-injured OHCs, but were not exposed to the blast overpressure.

Immunohistochemistry

At 2 h post injury, OHCs were fixed for 30 minutes (min) at room temperature (RT) with 4% paraformaldehyde (PFA) in 0.1 M phosphate buffer (PB) and immunohistochemistry (IHC) was performed [34]. At the time of fixation, OHCs were about 100 μm thick as they get thinner after a few days in culture [93–95]. Immunostaining with a polyclonal rabbit antibody against GFAP (Dako, Carpinteria, CA, USA Cat# Z0334, RRID: AB_2314535) was conducted directly on the insert membrane, which was cut out around the OHCs [34, 94, 96]. Additionally, OHCs that were pretreated with either Annexin V conjugated to Alexa 488 (ThermoFisher Scientific) or 10,000 kDa Dextran (Dex10) conjugated to Alexa 488 (ThermoFisher Scientific), as

described below, were gently peeled from the membrane insert and immunostained against GFAP (Dako) using the free-floating sections method [97]. Double labeling against GFAP (Dako) and glial glutamate transporter 1 (GLT-1; EMD Millipore Cat# AB1783, RRID: AB_90949) was also performed on the free-floating OHCs. Both OHCs attached to the insert membrane and free-floating sections were immunostained using the same protocol. Briefly, fixed OHCs were washed 3 times for 5 min in phosphate buffered saline (PBS) and incubated for 1 h at RT in blocking solution consisting of PBS, 5% normal goat serum (NGS; Thermo-Fisher Scientific), 5% bovine serum albumin (BSA; Sigma Aldrich, St. Louis, MO, USA) and 1% Triton-X 100 (TX-100; Sigma Aldrich). Following blocking, OHCs were incubated in GFAP (Dako) primary antibody diluted in blocking solution at 1:500 for 48 h at 4˚C in a humid atmosphere. For double staining, under the same conditions OHCs were simulta-neously incubated with polyclonal rabbit antibody against GFAP (Dako; 1:500) and polyclonal guinea pig antibody against GLT-1 (EMD Millipore; 1:1500). After washing, OHCs were incu-bated with appropriate secondary antibodies diluted in blocking solution without TX-100 as follows: Alexa Fluor 488 conjugated polyclonal goat anti-rabbit antibody (ThermoFisher Sci-entific Cat# A-11034, RRID:AB_2534092; 1:500), Alexa Fluor 647 conjugated polyclonal goat anti-rabbit antibody (ThermoFisher Scientific Cat# A-21245, RRID:AB_2535813; 1:750), and Alexa Fluor 488 conjugated polyclonal goat anti-guinea pig antibody (ThermoFisher Scientific Cat# A-11073, RRID:AB_2534117; 1:400). Staining specificity was confirmed by omission of primary antibody. Sections were counterstained with the nuclear dye DAPI (4', 6-diamindino-2-phenylindole dihydrochloride; Sigma-Aldrich) and mounted with VECTASHIELD HardSet mounting medium (Vector Laboratories, Burlingame, CA, USA). Immunostained OHCs were analyzed using a Leica TCS SP8 confocal laser scanning microscope (Leica Microsystems, Buf-falo Grove, IL, USA).

Quantification of dead astrocytes

The red fluorescent dye, PI (ThermoFisher Scientific) was used to assess cell death following blast injury [34, 98]. PI enters only into cells with a damaged cell membrane and is considered to be primarily a marker of necrotic cells [99]. OHCs were placed in media containing 2 μM PI [100, 101] for 2 h prior to imaging. All sections were imaged under identical conditions at prior to (basal) and 2 h following blast injury using a Nikon Eclipse TE2000-U upright fluores-cent microscope (Nikon Instrument Inc., Melville, NY, USA) equipped with a digital SPOT camera and software (Spot Imaging Solutions, Sterling Heights, MI, USA). Any OHC which had dissection or handling related damage prior to the beginning the experiment was excluded [84, 87, 88, 100]. Following PI imaging at 2 h post-injury, OHCs were fixed and processed for IHC as described above.

GFAP immunostained OHCs were used to acquire three non-overlapping images (290.63 μm by 290.63 μm) of the cornu Ammonis 1 (CA1) region by a Leica TCS SP8 confo-cal laser scanning microscope, and only a small fraction of CA1 region was not analyzed [34, 80]. Two observers blinded to the experimental groups counted in each image the total num-ber of dead astrocytes that were co-labeled for GFAP and PI. Counts obtained from the two observers were averaged and expressed as the total number of dead astrocytes per counting region [34]. The concordance correlation coefficient (CCC) was used to evaluate agreement among two observers.

Apoptosis assay

Annexin V binds with high affinity to membrane phospholipid phosphatidylserine (PS), which is transposed to the external side of the plasma membrane during early apoptosis [99,

102]. Accordingly, in our study Annexin V was used to assess the presence of apoptotic cells in OHCs in the acute phase of blast injury. Immediately following blast exposure, Annexin V conjugated to Alexa Fluor 488 (ThermoFisher Scientific Dead Cell Apoptosis Kit; 15 µl/ml) was added to the culture medium of control and OHCs exposed to blast overpressure. Simultaneously, OHCs were treated with PI (EMD Millipore; 2 µM). Following a 2 h incubation with Annexin V and PI, OHCs were fixed for 30 min at RT with 4% PFA in 0.1 M PB and immunostained against GFAP as described above.

Calpeptin treatment of OHCs

The calpain inhibitor calpeptin (Santa Cruz, Dallas, Texas, USA; 10 µM) [103] was added to the OHCs' serum-free medium followed immediately by a sham- or blast-injury. After the injury, samples were transferred to fresh serum-free medium containing the same concentration of calpeptin and PI (EMD Millipore; 2 µM). PI stained OHCs were imaged at 2 h postinjury and subsequently harvested for GFAP western blot analysis as described below.

Gel electrophoresis, western blot, and densitometry

For western blot analysis, 10 OHCs from two different inserts of the same experimental group were pooled to represent one sample [104]. Tissue was lysed in 300 µl lysis buffer consisting of 50 mM Tris-HCl, 150 mM NaCl, 1 mM ethylenediaminetetraacetic acid (EDTA), 0.1% sodium dodecyl sulfate (SDS), 1% Triton X-100, and 1% mammalian protease and phosphatase inhibitor cocktail [105] (All obtained from ThermoFisher Scientific, except for SDS which was obtained from Bio-Rad, Hercules, CA, USA, and Triton X-100 which was obtained from Sigma-Aldrich). Slice homogenates were prepared using a manual homogenizer (ThermoFisher Scientific), incubated on ice for 30 min, and were further centrifuged at 13,000 RPM for 20 min at 4˚C. The supernatant was collected and stored at -80˚C until use.

The protein concentration was determined by colorimetric detection with a bicinchoninic acid (BCA) assay (ThermoFisher Scientific) according to the manufacturer's protocol. Briefly, 10 µl of protein sample, or BSA standard, was loaded into a microplate. 200 µl of working solution was added to each sample and the microplate was incubated for 30 min at 37˚C. The absorbance was measured at 562 nm using a microplate reader (PowerWave XS, BioTek Instruments Inc., Winooski, VT).

For gel electrophoresis, samples were heated with laemmli Sample Buffer (Bio-Rad) and 100 mM of dithiothreitol (DTT; MidSci, Saint Louis, MO, USA) at 95˚C for 5 min. 15 µg/µl of sample protein was loaded onto a 10% Mini-PROTEAN TGX Stain-Free Precast Gel (Bio-Rad) and run under reducing conditions. The gel was blotted onto a polyvinylidene fluoride (PVDF) Immobilon ® FL membrane (EMD Millipore) via wet transfer. Following a brief wash in tris-buffered saline (TBS; pH 7.5), the membrane was blocked with 5% BSA in TBS supplemented with 0.05% Tween 20 (TTBS). Further, the membrane was probed with primary antibodies against GFAP (Dako; 1:10,000), calpain (Santa Cruz Cat# sc-373966, RRID: AB_10917913); 1:1,000) or GLT-1 (EMD Millipore; 1:20,000) at 4˚C overnight. Following a brief wash, membranes were incubated with goat anti-rabbit (ThermoFisher Scientific Cat# 31460, RRID: AB_228341; 1:10,000), goat anti mouse (ThermoFisher Scientific Cat# 31430, RRID: AB_228307; 1:10,000) or goat anti-guinea pig (ThermoFisher Scientific Cat# A18769, RRID: AB_2535546; 1:50,000) poly-horse radish peroxidase (HRP) conjugated secondary antibody diluted in blocking solution, respectively. A monoclonal antibody against mouse glyceraldehyde-3-phosphate dehydrogenase (GAPDH; Advanced Immunochemical, Long Beach, CA USA Cat# 6C5; 1:50,000) was used as a loading control with a

secondary goat anti-mouse (ThermoFisher Scientific; 1:50,000) HRP conjugated antibody. The membrane was then incubated with SuperSignal West Femto (ThermoFisher Scientific) for 5 min at RT and the signal was detected using a Carestream ECL 4000MM Pro imaging scanner (Carestream Inc., Rochester, NY, USA). Bands were scanned into digital images and analyzed by densitometry using Carestream Molecular Imaging Software Standard Edition v. 5.3.4.17821. Target band density was normalized to the appropriate loading control [106].

Assessment of altered membrane integrity following bTBI

Cell membrane disruption following blast exposure was evaluated using Alexa 488-conjugated Dex10, which is excluded from cells with an intact cell membrane [107, 108]. OHCs were incubated with Alexa 488-conjugated Dex10 (ThermoFisher Scientific; 0.02 mg/ml) from 2 h before injury until 2 h post-injury. Immediately following injury, PI (EMD Millipore; 2 μM) was also added to the OHCs' culture medium. Following imaging of PI staining at 2 h post-injury, OHCs were fixed and immunostained against GFAP as described above. To assess involvement of cell membrane perturbation in astrocytic cell death, co-labeling of GFAP, PI, and Dex10 was evaluated in mounted OHCs under TCS SP8 confocal laser scanning microscope (Leica Microsystems).

Data collection and statistical analysis

Quantification of dead astrocytes for each experimental group was performed on 5 OHCs obtained from at least 3 different animals. Three images in the CA1 region per section were acquired and were subsequently used for quantification of GFAP and PI co-labeled cells. Data are presented as the total number of dead astrocytes per counting area in the CA1 ± standard error of mean (SEM).

Western blot analysis for each protein was repeated on samples from at least 3 different experiments, with each sample consisting of 10 OHCs. Quantification of GLT-1- and GFAP-immuoreactive bands was performed using computer-assisted densitometry scanning. Data collected from 3 different samples per group were averaged and presented as arbitrary densitometry units of GLT-1 or GFAP relative to GAPDH loading control.

Statistical comparison among groups was done by one way analysis of variance (ANOVA) followed by a Tukey's *post hoc* test. A value of $P < 0.05$ was considered statistically significant.

Results

Acute astrocytic response to blast overpressure

At 2 h following OHCs' exposure to the blast overpressure, we have detected shearing, or tearing, of astrocytes as well as changes in their morphology, including swelling and beading, while astrocytes with mainly intact morphology were present in the sham control OHCs (Fig 1A–1C). In both the low- and the high-blast groups, we have observed clasmatodendrosis, which is defined by the beading and dissolution of astrocytic processes (Fig 1E and 1F). In OHCs exposed to a blast overpressure, clasmatodendrosis was present throughout the tissue (Fig 1E and 1F), whereas it was almost absent in the sham control group (Fig 1D). Moreover, at 2 h post-injury, we have observed in both the low- and high-blast groups a significant increase in the number of dead astrocytes, identified by co-labeling with the astrocytic marker GFAP and the cell death marker PI (Fig 1E amd 1F). Assessment of the number of dead astrocytes per counting region in the CA1(Fig 1G and 1H) had high
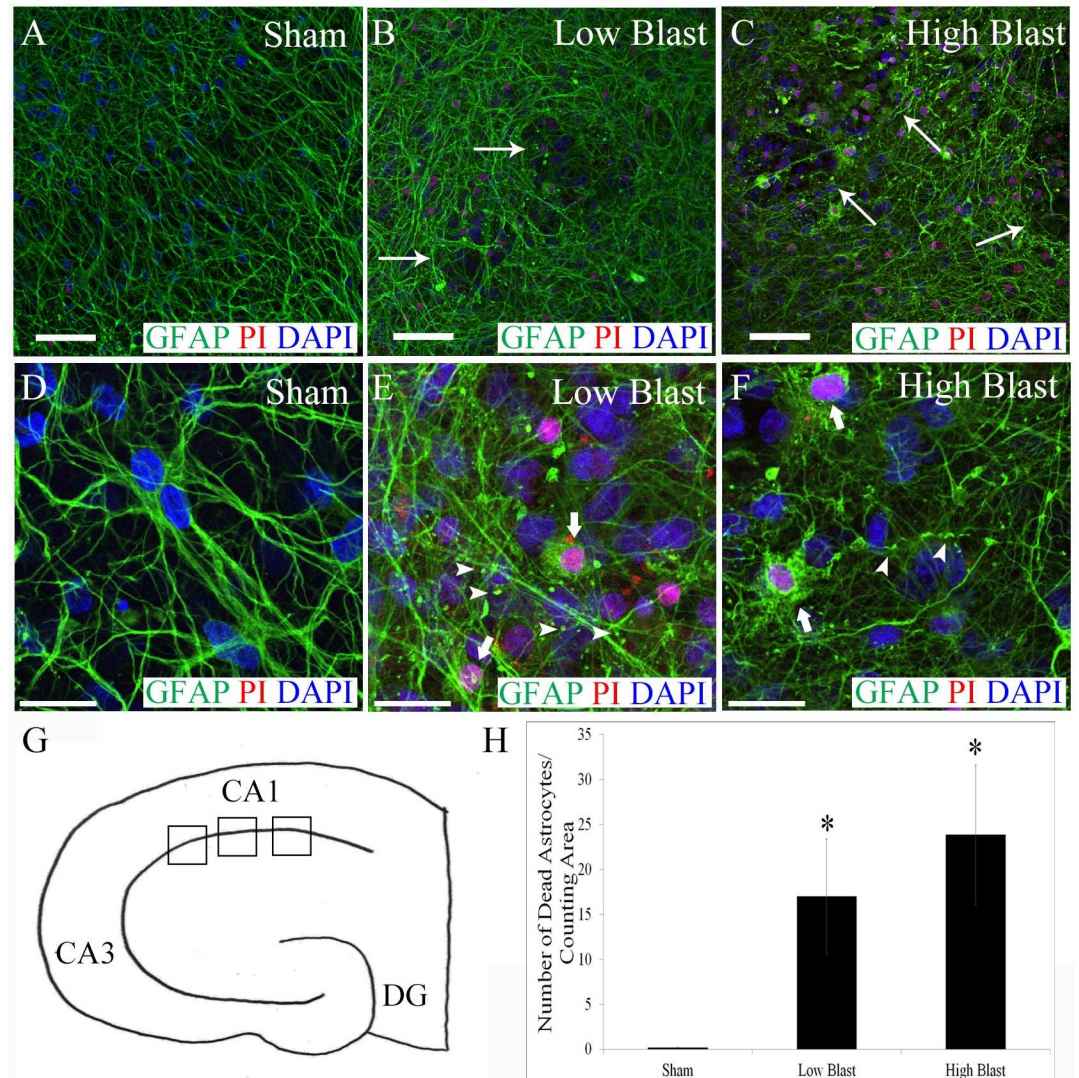
Fig 1. Acute morphological changes and demise of astrocytes following blast exposure. Representative confocal images acquired in the CA1 hippocampal region from sham controls (A, D), low-blast (B, E), and high-blast (C, F) OHCs that were fixed at 2 h following injury and stained with an anti-GFAP antibody (green), PI (red), and DAPI (blue). Shearing of the astrocytes (thin arrows) was detected in OHCs exposed to blast overpressure (B, C) while it was absent in the sham controls (A). Clasmatodendrosis (arrowheads) was also observed in the low- (E) and high-blast (F) groups, but it was very infrequent in the sham control group (D). At the same time point, only a few dead astrocytes were present in sham control OHCs (D) while significant number of dead astrocytes (thick arrows) was revealed in the low- (E) and high-blast (F) groups. (G) Schematic diagram of OHC, indicating approximate locations in the CA1 region (boxes) where images for quantification of dead astrocytes were taken. (H) Number of dead astrocytes per counting area in the CA1 hippocampal region at 2 h following injury was significantly higher in both the low- (*; $P < 0.05$; n = 5) and high-blast groups (*; $P < 0.05$; n = 5) compared to the sham control group (n = 5). Scale bars (A-C) 50 μm (D-F) 20 μm.

doi:10.1371/journal.pone.0173167.g001

interobserver agreement with the CCC of 0.9595. Quantitative data revealed a statistically significant increase in the number of dead astrocytes in the low- and high-blast compared to sham controls ($P < 0.05$) (Fig 1H). There was no statistically significant difference between the low- and high-blast groups; however there was a trend towards increased death of astrocytes in the high-blast group.
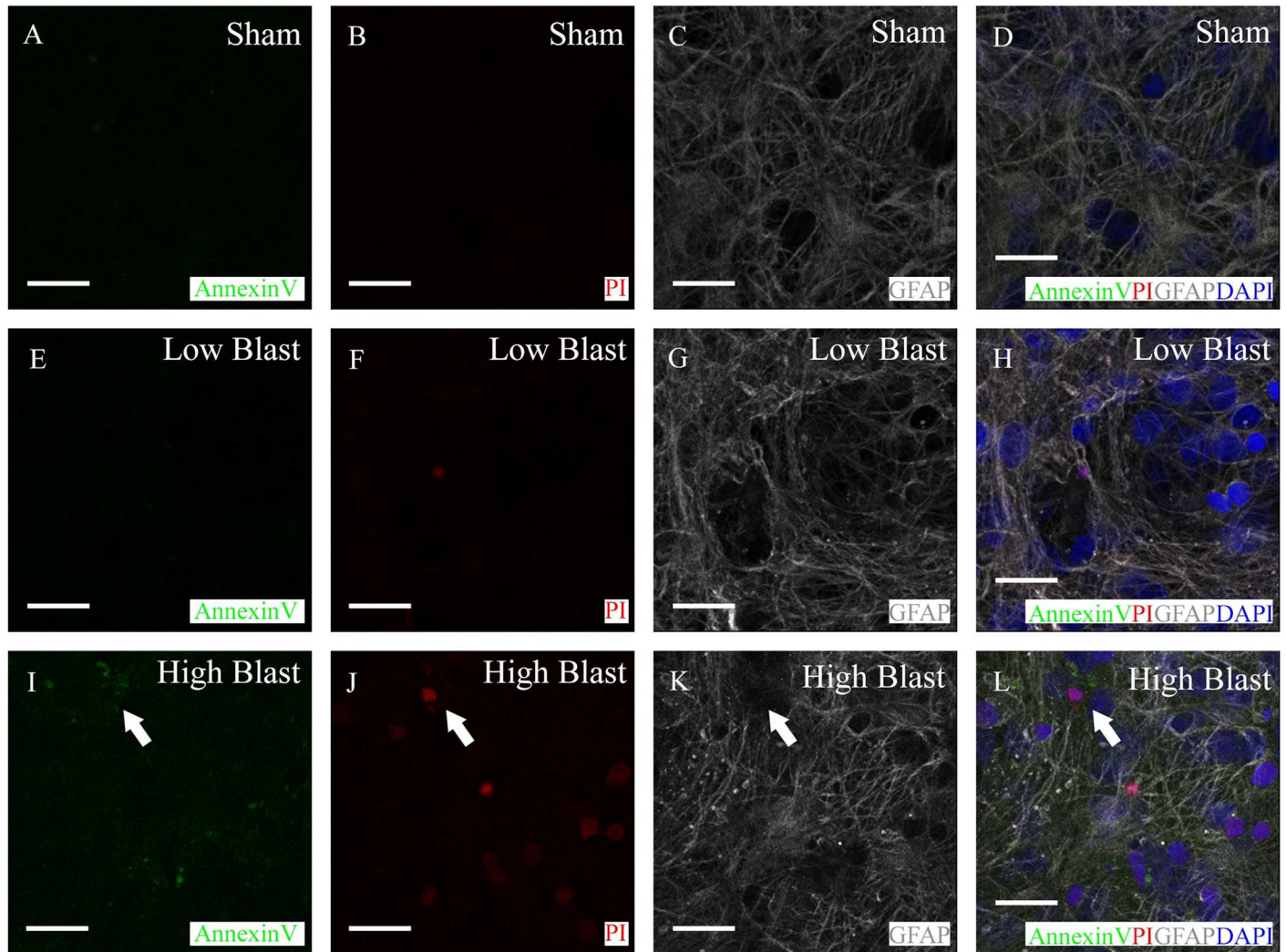
Fig 2. Limited early apoptotic death of astrocytes following blast exposure. At 2 h following injury, Annexin V conjugated to Alexa 488 (green; A, E, I) was used to identify apoptotic cells in sham control (A-D), low-blast (E-H), and high-blast (I-L) groups. Samples were additionally labeled with the cell death marker PI (red; B, F, J), an antibody against GFAP (gray; C, G, K), and DAPI (blue). Overlay of Annexin V, PI, GFAP, and DAPI staining (D, H, L). Annexin V positive cells (arrow) were infrequent in all three experimental groups. Almost none of the observed Annexin V positive cells were co-labeled with GFAP. Scale bars 20 μm.

doi:10.1371/journal.pone.0173167.g002

Infrequent astrocytic apoptosis in the early phase of blast injury

Staining with Alexa 488 conjugated Annexin V identified a small number of apoptotic cells in OHCs at 2 h following sham-, low-, and high-blast injury (Fig 2). In addition, almost none of the apoptotic, Annexin V positive cells were co-labeled with astrocytic marker GFAP (Fig 2).

Calpain mediated GFAP degradation in response to blast overpressure

Results from western blot analysis of both low- and high-blast groups at 2 h following injury revealed the presence of the full length astrocytic protein GFAP (50 kDa) and a range of GFAP break down products (GFAP-BDPs) down to 38 kDa (Fig 3A). At the same time point, only the full length GFAP (50 kDa) was observed in sham control OHCs (Fig 3A). Prevalently, expression of the calpain mediated 38 kDa GFAP-BDP [109] was increased in both the low-
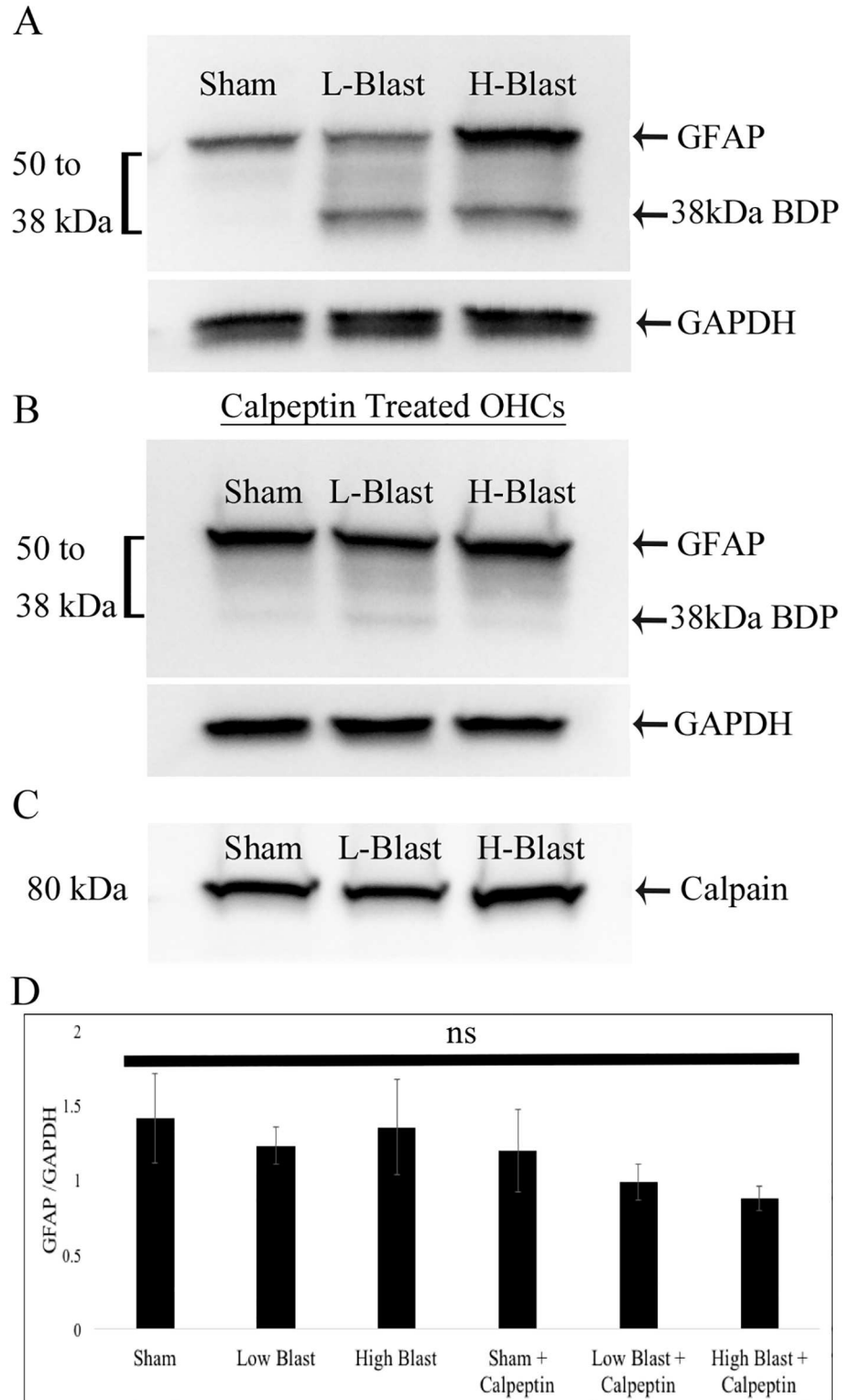
Fig 3. Calpain-mediated degradation of GFAP at 2 h following blast injury. Proteins were isolated from sham control (Sham), low-blast (L-Blast), and high-blast (H-Blast) OHCs at 2 h post-injury and analyzed via western blot for expression of GFAP (A, B) or calpain (C). (A) The 38 kDa calpain associated GFAP-BDP was present in blast-injured OHCs, but not in corresponding sham control OHCs. (B) Following inhibition of calpain via calpeptin treatment, this GFAP-BDP at 38 kDa was not observed. (C) Calpain expression in OHCs exposed to blast overpressure compared to sham controls was not changed at this time point. (D)

Densitometry analysis of GFAP 50 kDa/GAPDH ratio for 3 independent experiments revealed no significant (ns) differences among control and blast-exposed OHCs without or with calpeptin treatment.

and high- blast overpressure exposure groups (Fig 3A). Moreover, treatment with the calpain inhibitor calpeptin prevented the generation of the 38 kDa GFAP-BDP in OHCs at 2 h following blast injury (Fig 3B). However, western blot analyses revealed similar expression levels of calpain in all experimental groups (Fig 3C). In addition, densitometry analysis demonstrated that expression levels of full length GFAP were not significantly different among experimental groups with or withouth calpeptin treatment (Fig 3D).

Acute astrocytic membrane disruption following blast exposure

The effect of a blast overpressure on membrane permeability was studied in OHCs at 2 h following injury using a Dex10 conjugated to Alexa 488 infusion tracer [107, 108]. Additionally, Dex10 treated OHCs were co-labeled with the cell death marker PI and the astrocytic marker GFAP (Fig 4). We have observed an increase in the number of dextran positive cells at 2 h following injury in the low- and high-blast groups compared to the sham controls (Fig 4). Moreover, a fraction of Dex10 positive cells co-expressed PI and GFAP at 2 h following blast injury (Fig 4).

Acute demise of GLT-1-expressing astrocytes

Double labeling for GFAP and GLT-1 demonstrated significant loss of GLT-1 expressing astrocytes (Fig 5A–1C), implying decreased glutamate uptake following bTBI. However, western blot assay for GLT-1 expression levels (Fig 5D) followed by densitometry analyses (Fig 5E), did not demonstrate significant differences between sham control, low-, and high-blast OHCs at 2 h post-injury.

Discussion

Given the recent rise in the incidence of bTBI [1–4], it is paramount to elucidate mechanisms underlying blast-evoked cell death and develop effective neuroprotective interventions. This
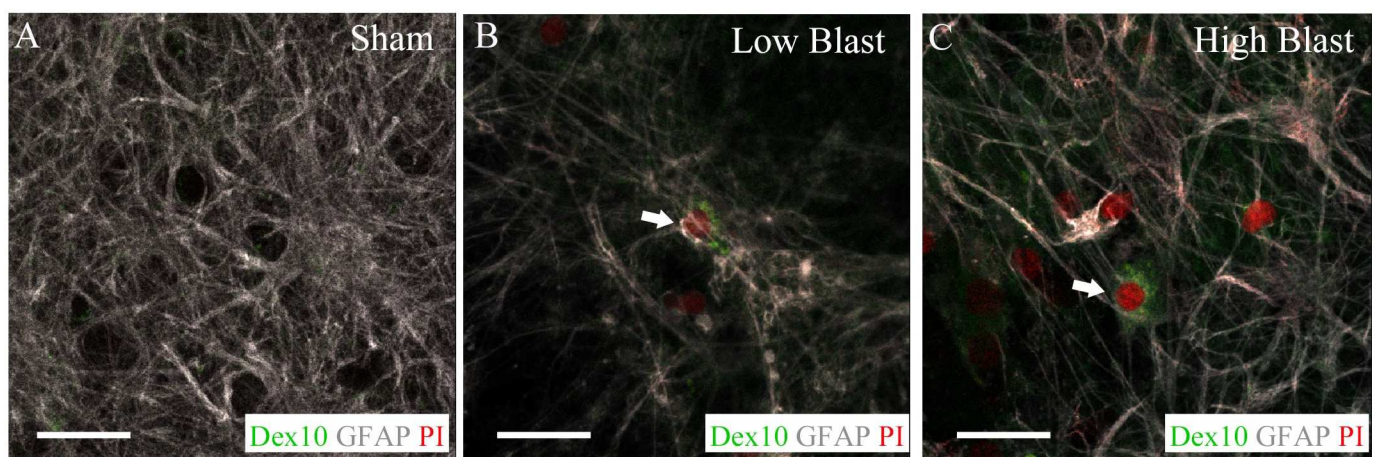
Fig 4. Increased astrocytic membrane permeability at 2 h post injury. Dex10 (green) and PI (red) labeled sham control (A), low-blast (B), or high-blast (C) OHCs were fixed 2 h following injury and further stained with an anti-GFAP antibody (gray). Dead astrocytes with increased membrane permeability, identified by overlap of GFAP, PI, and Dex10 staining (arrows), were only present in the low-blast (B) and high-blast (C) OHCs but not in the sham controls (A). Scale bars 20 μm.
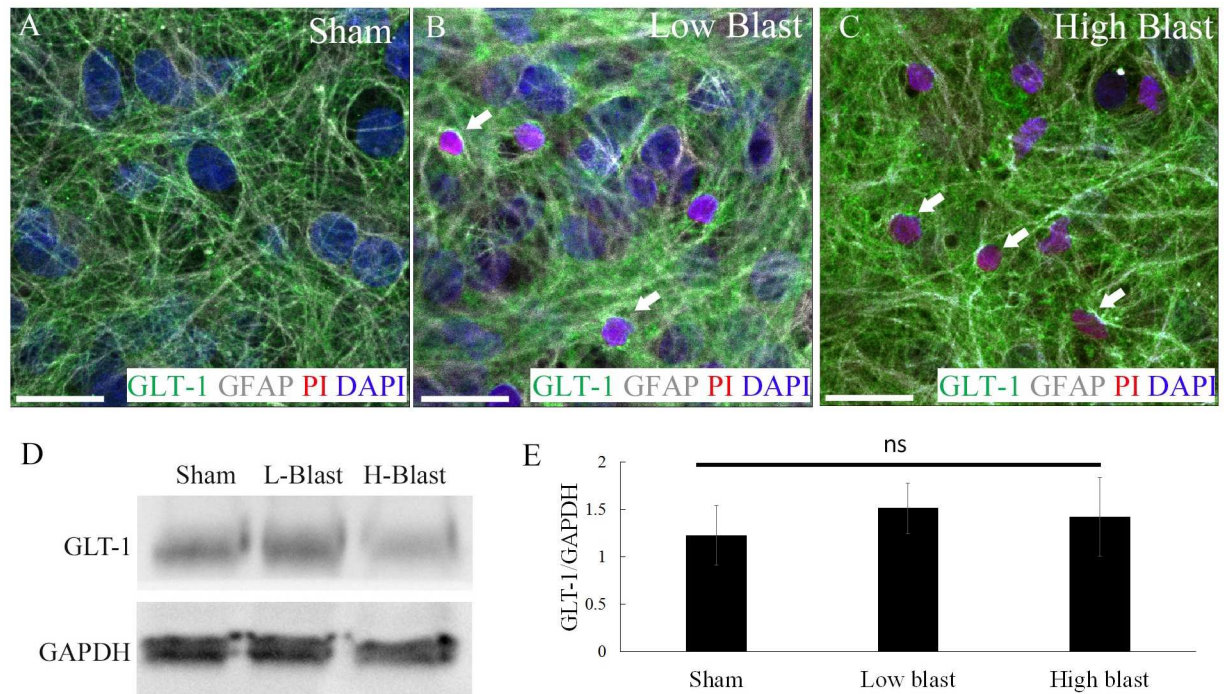
Fig 5. Blast-induced loss of GLT-1-expressing astrocytes. At 2 h following injury, sham control (A), low-blast (B), and high-blast (C) OHCs were stained using antibodies against GLT-1 (green), GFAP (gray), PI (red), and DAPI (blue). Dead astrocytes, identified by co-labeling of GFAP and PI (arrows) were also positive for GLT-1. (D) Representative immunoblot analyses of GLT-1 protein expression in sham control (Sham) and OHCs exposed to blast overpressure (L-Blast and H-Blast). (E) Densitometry analysis of GLT-1/GAPDH ratio for 3 independent experiments revealed no significant (ns) differences between sham control, low-blast, and high blast groups. Scale bars 20 μm.

doi:10.1371/journal.pone.0173167.g005

study determined acute effects of blast exposure on astrocytes and depicted mechanisms of blast-evoked astrocytic death in an *in vitro* bTBI model. We demonstrated that blast exposure has a profound effect on astrocytes acutely following injury in both the low- and high-blast groups compared to sham controls. Our main findings included a statistically significant increase in necrotic astrocytic death in both low- and high-blast groups compared to sham controls. Additionally, our data suggest calpain mediated GFAP breakdown and increased plasmalemmal permeability as mechanisms of blast-evoked astrocytic death, and further implies glutamate dysregulation following bTBI.

We previously validated an OHC-based *in vitro* bTBI model as a tool to study cellular and molecular changes following blast exposure [34]. Advantages of OHCs cultures include preservation of 3D tissue-specific cytoarchitecture, neuronal-glial interactions, as well as interregional neuronal connectivity of an *in vivo* hippocampus [83, 93, 110]. One potential limitation is that OHCs are typically prepared from postnatal donors, as these cultures survive better [93, 95, 111]. However, OHCs prepared from neonatal donors gain more mature phenotype over the first few weeks of culture [95, 112, 113] and display similar gene regulation, protein expression, and synaptic activity of the adult hippocampus [111, 114, 115]. We cannot exclude that due to the absence of active circulatory system, bones of the scull, inputs from extra hippocampal brain regions, and systemic response in our *in vitro* bTBI model, cellular response and it's temporal profile could be somewhat different compared to *in vivo* situation. However, previous studies demonstrated that primary and secondary cell death, as well as temporal course of damage and changes in cell death genes in OHCs exposed to mechanical or ischemic injury

are similar to those observed *in vivo* [84, 116–118]. Despite limitations, there are clear benefits to the OHC reductionism and they have been extensively used to model blast and non-blast TBI [32, 33, 84, 85, 118–120].

To generate *in vitro* bTBI model, as in our previous studies [34], culture dishes with OHCs were placed outside of the shock tube and positioned 55° off axis to avoid effects of exhaust gases resulting in complex shock waves [121, 122]. OHCs were exposed to blast overpressures of approximately 150 and 280 kPa, that in our previous *in vitro* study evoked significant cell death [34]. Experimental designs similar to ours were implemented in several recent *in vitro* [32, 33, 119, 120, 123, 124] and *in vivo* bTBI studies [19, 122, 125, 126]. Notably, our shock tube model for rats [16, 28, 127] is quite similar to the model presented in this study, including design, peak overpressure and positive duration. Using the present design, it should be noted that this loading condition can be a combination of primary (shock wave overpressure) and possible tertiary loading due to acoustic impedance mismatch between the different materials (e.g., air, well, medium) that may have resulted in inertial loading that may have led to mechanical deformation (i.e., strain) of the tissue sample [34].

In the present study we analyzed cellular changes in OHCs at 2 h following blast exposure, as under the same conditions we previously observed dramatic increase in cell death from 0 to 2 h post-injury [34]. At 2 h post-injury, in addition to dead astrocytes we also observed dead neurons and microglial cells (data not shown). However, we focused our analyses on the vigorous early astrocytic response to blast overpressure that was not previously reported. In our earlier studies we demonstrated robust activation of astrocytes at 72 h post injury, however at that time point we detected only a small number of dead astrocytes [34]. Though, corresponding to our current results, we observed dead microglial cells at 4 and 24 h post-injury [34]. Collectively, results from our present and previous studies show acute astrocytic demise followed by robust activation at 72 h post-injury. Similar to our data, astrocytic damage and PI uptake was observed in the stretch-injury model only immediately following injury, but not at the 24 and 48 h post-injury [128, 129]. Correspondingly, results collected from human blunt TBI cases implied that number of astrocytes initially decreases within the first 24 h post-injury and then again increases at the later time points, indicating formation of reactive gliosis [76]. However, significant changes in viability of astrocytes were not observed in astrocyte monocultures exposed to the blast overpressure [130, 131]. Assessments were conducted only at later time points post-injury, which could explain why initial astrocytic susceptibility was not observed. Moreover, blast shock wave may not have the same biological effects in astrocyte monocultures as in OHCs that more closely resemble *in vivo* situation [83, 93, 110]. In agreement with our data, death of astrocytes [67, 78] and their activation [35, 66, 67, 125, 132, 133] were detected in animal studies following shock wave exposure. On the contrary, several *in vivo* bTBI studies did not observe increased GFAP expression [134–136], which could be due to the different experimental conditions and assessment timing.

In this study we observed significant co-labeling of GFAP-expressing astrocytes with the cell death marker PI, which identified necrosis as the primary mechanism of astrocytic death in OHCs at 2 h following blast exposure. Additionally, we studied presence of apoptotic astrocytes in the acute phase of bTBI using co-labeling with Annexin V and GFAP. Fluorescently labeled Annexin V was previously used in OHCs and different *in vivo* models of brain injury [137–139] to detect apoptotic cells even within several hours following injury [140–142]. The limited detection of Annexin V positive cells at 2 h following blast exposure, rules out apoptosis as a significant contributing factor to astrocytic death acutely following blast exposure. It was previously shown that both necrotic and apoptotic cell death are implicated in bTBI [133, 143–145]. Studies in monkey [67] and rat [78] bTBI models detected apoptotic astrocytes at 1 month and 1 day post-injury, respectively. However, those studies did not assess astrocytic

apoptotic death at more acute time points as we did. Therefore, our data together with results collected in *in vivo* bTBI models [67, 78] imply that apoptosis may play a significant role in astrocytic death at later time points.

Beside the acute death, we observed blast-evoked shearing and morphological changes in astrocytes. Clasmatodendrosis, an irreversible astroglial degeneration characterized by beading and dissolution of their processes [146], was also observed at 2 h following injury. In accordance with our results, other groups demonstrated that shock waves can generate shear forces in the brain tissue [25, 132, 147] and induce elongation and deformation of the cell organelles [25, 145, 148]. Trauma-induced morphological changes of astrocytes, such as swelling and ultrastructural alterations, were previously perceived in an *in vitro* model of fluid percussion injury [149, 150], stretched-injured astrocytes [151], a rat bTBI model [152], and in patients with cerebral contusions [77, 153]. Likewise, clasmatodendrosis of astrocytes was detected in TBI patients from 1 h up to 14 days post injury [154]. Clasmatodendrosis in astrocytes was linked with the autophagic cell death [155, 156], suggesting autophagy as an additional mechanism of astrocytic death in OHCs at 2 h following blast exposure. Accordingly, an increase in autophagy that can lead to cell death was previously observed following blunt TBI [157–160] and bTBI [23].

Furthermore, our study revealed cleavage of GFAP by calpain as a potential mechanism of early astrocytic death, based on the presence of calpain-mediated 38 kDa GFAP-BDP at 2 h following injury. Moreover, when we introduced the calpain inhibitor calpeptin into the OHCs culture medium, formation of the 38 kDa GFAP-BDP in the blast-injured groups was prevented, while expression levels of full length GFAP remained similar. Expression levels of calpain were similar in all experimental groups, suggesting only increase in calpain activity following blast exposure due to the calcium overload [161]. Previous human and animal studies established that calpains play a key role in neuropathological changes following blunt TBI and that application of calpain-inhibitors can have protective effects [109, 162–164]. Recent studies in a mouse bTBI model also reported increased calpain-mediated cytoskeletal breakdown [165, 166]. Corresponding to our data, it has been shown that beside neuronal proteins, GFAP can be calpain substrate as well [109, 167]. In addition, it has been shown that both increased serum levels of GFAP [168–170] and GFAP-BDPs [109, 171–173] are strong biomarkers of brain injury.

The overlap of Dex10, GFAP, and PI staining observed in the present study in low-and high-blast groups, indicated plasmalemmal disruption as an additional mechanism of astrocytic death in response to the blast overpressure at 2 h following injury. In addition, a fraction of Dex10-labeled cells in OHCs exposed to blast overpressure did not express GFAP, implying that blast exposure also causes rapid changes in cell membrane permeability in other cell types in OHCs. Complex changes in cell membrane permeability that can lead to the ionic imbalances and activation of several cellular pathways have been previously described in stretched-injured astrocytes [129, 174, 175], as well as in blunt and diffuse TBI models [107, 108, 176, 177]. In addition, increased cell permeability and cytoskeletal damage has been observed following blast exposure in the dorsal root ganglion (DRG) [178] and SH-SY5Y human neuroblastoma cells [31]. Correspondingly, acute decrease in GFAP/Tau was detected in the mouse brain after blast exposure, which most likely was result of blast-induced perturbation of neuronal and astrocytic cell membranes and protein leakage across the disrupted blood-brain barrier [179].

Based on the essential role of astrocytes in maintaining brain homeostasis, it is feasible that the acute death of astrocytes observed in our studies could be implicated in secondary neuronal loss following bTBI. A link between acute astrocytic death and delayed neuronal loss has also been postulated in models of ischemic and blunt brain injury [59, 74]. Despite no

apparent changes in GLT-1 protein expression, significant loss of GLT-1 expressing astrocytes observed in our studies at 2 h following blast injury, implies a reduction of glutamate uptake that can further cause excitotoxic neuronl and glial death [180–183]. Under normal physiological conditions, astrocytes regulate extracellular glutamate concentration through release and transport via glutamate transporters [37, 54, 184, 185]. Out of five sodium-dependent glutamate transporters that have been cloned [185], GLT-1 is responsible for the majority of glutamate uptake [186, 187] and it is mainly expressed by astrocytes [188]. However, neurons and microglial cells also express GLT-1 [75, 188, 189] and it is feasible that blast-evoked loss of these cells could be also implicated in the disruption of glutamate uptake. In addition, previous studies demonstrated that both excessive glutamate release from neurons and dysfunction of astrocytes could contribute to a prompt increase of extracellular glutamate concentration following TBI [182, 190, 191]. Likewise, several studies reported decrease in GLT-1 expression in blunt TBI models [75, 192, 193] and in human TBI [76]. In our previous studies we have demonstrated the spread of cell death following bTBI and that at 72 h post-injury majority of dead cells were neurons [34]. Based on data from this study, we speculate that early demise of astrocytes and potential glutamate dysregulation could aggravate neuronal loss at the later time points post-injury.

In conclusion, this study demonstrated substantial acute effects of blast overpressure on astrocytes in OHCs. Understanding the damage incurred by astrocytes at 2 h post-injury in this *in vitro* model paves a path for understanding the role of astrocytes in bTBI neuropathology. Results presented here provide steps toward future research, which will examine whether the acute astrocytic demise significantly contributes to the delayed neuronal loss and whether astrocytes could be targeted to prevent spread of neurodegeneration following bTBI.

Acknowledgments

Author Contributions

Conceptualization: AGJ BDS APM SNK.

Data curation: APM BVA ASS AGJ.

Formal analysis: APM AGJ ASS BVA.

Funding acquisition: AGJ BDS SNK.

Investigation: APM BVA ASS AGJ.

Methodology: AGJ BDS APM ASS BVA.

Project administration: AGJ BDS.

Resources: APM BVA ASS AGJ BDS.

Supervision: AGJ BDS SNK.

Validation: AGJ BDS APM ASS BVA.

Visualization: APM AGJ.

Writing – original draft: APM AGJ.

Writing – review & editing: AGJ APM BDS BVA ASS SNK.

References

1. Owens BD, Kragh JF Jr., Wenke JC, Macaitis J, Wade CE, Holcomb JB. Combat wounds in operation Iraqi Freedom and operation Enduring Freedom. The Journal of trauma. 2008; 64(2):295–9. Epub 2008/02/28. doi: 10.1097/TA.0b013e318163b875 PMID: 18301189

2. Warden D. Military TBI during the Iraq and Afghanistan wars. The Journal of head trauma rehabilitation. 2006; 21(5):398–402. Epub 2006/09/20. PMID: 16983225

3. Shively SB, Perl DP. Traumatic brain injury, shell shock, and posttraumatic stress disorder in the military—past, present, and future. The Journal of head trauma rehabilitation. 2012; 27(3):234–9. Epub 2012/05/11. PMID: 22573042

4. Bell RS, Vo AH, Neal CJ, Tigno J, Roberts R, Mossop C, et al. Military traumatic brain and spinal column injury: a 5-year study of the impact blast and other military grade weaponry on the central nervous system. The Journal of trauma. 2009; 66(4 Suppl):S104–11. Epub 2009/06/12. doi: 10.1097/TA.0b013e31819d88c8 PMID: 19359953

5. Ling G, Bandak F, Armonda R, Grant G, Ecklund J. Explosive blast neurotrauma. Journal of neurotrauma. 2009; 26(6):815–25. Epub 2009/04/29. doi: 10.1089/neu.2007.0484 PMID: 19397423

6. Terrio H, Brenner LA, Ivins BJ, Cho JM, Helmick K, Schwab K, et al. Traumatic brain injury screening: preliminary findings in a US Army Brigade Combat Team. The Journal of head trauma rehabilitation. 2009; 24(1):14–23. Epub 2009/01/23. PMID: 19158592

7. Bogdanova Y, Verfaellie M. Cognitive sequelae of blast-induced traumatic brain injury: recovery and rehabilitation. Neuropsychology review. 2012; 22(1):4–20. Epub 2012/02/22. doi: 10.1007/s11065-012-9192-3 PMID: 22350691

8. Magnuson J, Leonessa F, Ling GS. Neuropathology of explosive blast traumatic brain injury. Current neurology and neuroscience reports. 2012; 12(5):570–9. Epub 2012/07/28. doi: 10.1007/s11910-012-0303-6 PMID: 22836523

9. Kobeissy F, Mondello S, Tumer N, Toklu HZ, Whidden MA, Kirichenko N, et al. Assessing Neuro-Systemic & Behavioral Components in the Pathophysiology of Blast-Related Brain Injury. Frontiers in neurology. 2013; 4:186. Epub 2013/12/07. doi: 10.3389/fneur.2013.00186 PMID: 24312074

10. Macdonald CL, Johnson AM, Nelson EC, Werner NJ, Fang R, Flaherty SF, et al. Functional Status after Blast-Plus-Impact Complex Concussive Traumatic Brain Injury in Evacuated United States Military Personnel. Journal of neurotrauma. 2014. Epub 2013/12/26.

11. Rigg JL, Mooney SR. Concussions and the military: issues specific to service members. PM & R: the journal of injury, function, and rehabilitation. 2011; 3(10 Suppl 2):S380–6. Epub 2011/11/09.

12. Tanielian T, Jaycox LH. Invisible wounds of war: psychological and cognitive injuries, their consequences, and services to assist recovery. Rand Corp: Santa Monica, CA. 2008.

13. Mendez MF, Owens EM, Reza Berenji G, Peppers DC, Liang LJ, Licht EA. Mild traumatic brain injury from primary blast vs. blunt forces: post-concussion consequences and functional neuroimaging. NeuroRehabilitation. 2013; 32(2):397–407. Epub 2013/03/29. doi: 10.3233/NRE-130861 PMID: 23535805

14. Hoffer ME, Donaldson C, Gottshall KR, Balaban C, Balough BJ. Blunt and blast head trauma: different entities. Int Tinnitus J. 2009; 15(2):115–8. PMID: 20420334

15. Ibolja Cernak FA A. A comparative analysis of blast-induced neurotrauma and blunt traumatic brain injury reveals significant differences in injury mechansims. Medical Data. 2010; 2(4):297–304. Epub December 2010.

16. Stemper BD, Shah AS, Budde MD, Olsen CM, Glavaski-Joksimovic A, Kurpad SN, et al. Behavioral Outcomes Differ between Rotational Acceleration and Blast Mechanisms of Mild Traumatic Brain Injury. Frontiers in neurology. 2016; 7:31. doi: 10.3389/fneur.2016.00031 PMID: 27014184

17. Clemedson CJ. Blast injury. Physiological reviews. 1956; 36(3):336–54. Epub 1956/07/01. PMID: 13359127

18. Cernak I, Wang Z, Jiang J, Bian X, Savic J. Ultrastructural and functional characteristics of blast injury-induced neurotrauma. The Journal of trauma. 2001; 50(4):695–706. Epub 2001/04/17. PMID: 11303167

19. Long JB, Bentley TL, Wessner KA, Cerone C, Sweeney S, Bauman RA. Blast overpressure in rats: recreating a battlefield injury in the laboratory. Journal of neurotrauma. 2009; 26(6):827–40. Epub 2009/04/29. doi: 10.1089/neu.2008.0748 PMID: 19397422

20. Moss WC, King MJ, Blackman EG. Skull flexure from blast waves: a mechanism for brain injury with implications for helmet design. Physical review letters. 2009; 103(10):108702. Epub 2009/10/02. doi: 10.1103/PhysRevLett.103.108702 PMID: 19792349

21. Cernak I, Noble-Haeusslein LJ. Traumatic brain injury: an overview of pathobiology with emphasis on military populations. Journal of cerebral blood flow and metabolism: official journal of the International Society of Cerebral Blood Flow and Metabolism. 2010; 30(2):255–66. Epub 2009/10/08.

22. Courtney AC, Courtney MW. A thoracic mechanism of mild traumatic brain injury due to blast pressure waves. Medical hypotheses. 2009; 72(1):76–83. doi: 10.1016/j.mehy.2008.08.015 PMID: 18829180

23. Goldstein LE, Fisher AM, Tagge CA, Zhang XL, Velisek L, Sullivan JA, et al. Chronic traumatic encephalopathy in blast-exposed military veterans and a blast neurotrauma mouse model. Science translational medicine. 2012; 4(134):134ra60. Epub 2012/05/18. doi: 10.1126/scitranslmed.3003716 PMID: 22593173

24. Bauman RA, Ling G, Tong L, Januszkiewicz A, Agoston D, Delanerolle N, et al. An introductory characterization of a combat-casualty-care relevant swine model of closed head injury resulting from exposure to explosive blast. Journal of neurotrauma. 2009; 26(6):841–60. Epub 2009/02/14. doi: 10.1089/neu.2009-0898 PMID: 19215189

25. Nakagawa A, Manley GT, Gean AD, Ohtani K, Armonda R, Tsukamoto A, et al. Mechanisms of primary blast-induced traumatic brain injury: insights from shock-wave research. Journal of neurotrauma. 2011; 28(6):1101–19. Epub 2011/02/22. doi: 10.1089/neu.2010.1442 PMID: 21332411

26. Saljo A, Mayorga M, Bolouri H, Svensson B, Hamberger A. Mechanisms and pathophysiology of the low-level blast brain injury in animal models. NeuroImage. 2011; 54 Suppl 1:S83–8.

27. Shah AS, Stemper BD, Pintar FA. Development and characterization of an open-ended shock tube for the study of blast mTBI. Biomed Sci Instrum. 2012; 48:1–6.

28. Budde MD, Shah A, McCrea M, Cullinan WE, Pintar FA, Stemper BD. Primary blast traumatic brain injury in the rat: relating diffusion tensor imaging and behavior. Frontiers in neurology. 2013; 4:154. Epub 2013/10/18. doi: 10.3389/fneur.2013.00154 PMID: 24133481

29. Shah AS, Stemper BD, Yoganandan N, Pintar FA, Rangarajan N, Hallman J, et al. Methodology to study attenuation of a blast wave through the cranium. The American Society of Mechanical Engineers 2011 International Mechanical Engineering Congress and Exposition. 2011;17–24.

30. Arun P, Spadaro J, John J, Gharavi RB, Bentley TB, Nambiar MP. Studies on blast traumatic brain injury using in-vitro model with shock tube. Neuroreport. 2011; 22(8):379–84. Epub 2011/05/03. doi: 10.1097/WNR.0b013e328346b138 PMID: 21532394

31. Arun P, Abu-Taleb R, Valiyaveettil M, Wang Y, Long JB, Nambiar MP. Transient changes in neuronal cell membrane permeability after blast exposure. Neuroreport. 2012; 23(6):342–6. Epub 2012/03/20. doi: 10.1097/WNR.0b013e328351b58d PMID: 22426026

32. Effgen GB, Hue CD, Vogel E 3rd, Panzer MB, Meaney DF, Bass CR, et al. A Multiscale Approach to Blast Neurotrauma Modeling: Part II: Methodology for Inducing Blast Injury to in vitro Models. Frontiers in neurology. 2012; 3:23. Epub 2012/03/01. doi: 10.3389/fneur.2012.00023 PMID: 22375134

33. Effgen GB, Vogel EW 3rd, Lynch KA, Lobel A, Hue CD, Meaney DF, et al. Isolated primary blast alters neuronal function with minimal cell death in organotypic hippocampal slice cultures. Journal of neurotrauma. 2014; 31(13):1202–10. doi: 10.1089/neu.2013.3227 PMID: 24558968

34. Miller AP, Shah AS, Aperi BV, Budde MD, Pintar FA, Tarima S, et al. Effects of blast overpressure on neurons and glial cells in rat organotypic hippocampal slice cultures. Frontiers in neurology. 2015; 6:20. doi: 10.3389/fneur.2015.00020 PMID: 25729377

35. Svetlov SI, Prima V, Kirk DR, Gutierrez H, Curley KC, Hayes RL, et al. Morphologic and biochemical characterization of brain injury in a model of controlled blast overpressure exposure. The Journal of trauma. 2010; 69(4):795–804. Epub 2010/03/11. doi: 10.1097/TA.0b013e3181bbd885 PMID: 20215974

36. Saljo A, Bao F, Haglid KG, Hansson HA. Blast exposure causes redistribution of phosphorylated neurofilament subunits in neurons of the adult rat brain. Journal of neurotrauma. 2000; 17(8):719–26. Epub 2000/09/06. doi: 10.1089/089771500415454 PMID: 10972247

37. Maragakis NJ, Rothstein JD. Mechanisms of Disease: astrocytes in neurodegenerative disease. Nat Clin Pract Neurol. 2006; 2(12):679–89. doi: 10.1038/ncpneuro0355 PMID: 17117171

38. Rossi D, Volterra A. Astrocytic dysfunction: insights on the role in neurodegeneration. Brain Res Bull. 2009; 80(4–5):224–32. doi: 10.1016/j.brainresbull.2009.07.012 PMID: 19631259

39. Heales SJ, Lam AA, Duncan AJ, Land JM. Neurodegeneration or neuroprotection: the pivotal role of astrocytes. Neurochem Res. 2004; 29(3):513–9. PMID: 15038599

40. Burda JE, Bernstein AM, Sofroniew MV. Astrocyte roles in traumatic brain injury. Exp Neurol. 2015.

41. Floyd CL, Lyeth BG. Astroglia: important mediators of traumatic brain injury. Prog Brain Res. 2007; 161:61–79. doi: 10.1016/S0079-6123(06)61005-4 PMID: 17618970

42. Takano T, Tian GF, Peng W, Lou N, Libionka W, Han X, et al. Astrocyte-mediated control of cerebral blood flow. Nat Neurosci. 2006; 9(2):260–7. doi: 10.1038/nn1623 PMID: 16388306

43. Simard M, Nedergaard M. The neurobiology of glia in the context of water and ion homeostasis. Neuroscience. 2004; 129(4):877–96. doi: 10.1016/j.neuroscience.2004.09.053 PMID: 15561405

44. Ye ZC, Wyeth MS, Baltan-Tekkok S, Ransom BR. Functional hemichannels in astrocytes: a novel mechanism of glutamate release. J Neurosci. 2003; 23(9):3588–96. PMID: 12736329

45. Choi HB, Gordon GR, Zhou N, Tai C, Rungta RL, Martinez J, et al. Metabolic communication between astrocytes and neurons via bicarbonate-responsive soluble adenylyl cyclase. Neuron. 2012; 75(6):1094–104. doi: 10.1016/j.neuron.2012.08.032 PMID: 22998876

46. Pellerin L, Bouzier-Sore AK, Aubert A, Serres S, Merle M, Costalat R, et al. Activity-dependent regulation of energy metabolism by astrocytes: an update. Glia. 2007; 55(12):1251–62. doi: 10.1002/glia.20528 PMID: 17659524

47. Schousboe A, Bak LK, Waagepetersen HS. Astrocytic Control of Biosynthesis and Turnover of the Neurotransmitters Glutamate and GABA. Front Endocrinol (Lausanne). 2013; 4:102.

48. Volterra A, Meldolesi J. Astrocytes, from brain glue to communication elements: the revolution continues. Nat Rev Neurosci. 2005; 6(8):626–40. doi: 10.1038/nrn1722 PMID: 16025096

49. Haydon PG, Carmignoto G. Astrocyte control of synaptic transmission and neurovascular coupling. Physiol Rev. 2006; 86(3):1009–31. doi: 10.1152/physrev.00049.2005 PMID: 16816144

50. Christopherson KS, Ullian EM, Stokes CC, Mullowney CE, Hell JW, Agah A, et al. Thrombospondins are astrocyte-secreted proteins that promote CNS synaptogenesis. Cell. 2005; 120(3):421–33. doi: 10.1016/j.cell.2004.12.020 PMID: 15707899

51. Eroglu C, Barres BA. Regulation of synaptic connectivity by glia. Nature. 2010; 468(7321):223–31. doi: 10.1038/nature09612 PMID: 21068831

52. Jeremic A, Jeftinija K, Stevanovic J, Glavaski A, Jeftinija S. ATP stimulates calcium-dependent glutamate release from cultured astrocytes. J Neurochem. 2001; 77(2):664–75. PMID: 11299329

53. Parpura V, Basarsky TA, Liu F, Jeftinija K, Jeftinija S, Haydon PG. Glutamate-mediated astrocyte-neuron signalling. Nature. 1994; 369(6483):744–7. doi: 10.1038/369744a0 PMID: 7911978

54. Jeftinija SD, Jeftinija KV, Stefanovic G, Liu F. Neuroligand-evoked calcium-dependent release of excitatory amino acids from cultured astrocytes. J Neurochem. 1996; 66(2):676–84. PMID: 8592139

55. Giffard RG, Swanson RA. Ischemia-induced programmed cell death in astrocytes. Glia. 2005; 50 (4):299–306. doi: 10.1002/glia.20167 PMID: 15846803

56. Mouser PE, Head E, Ha KH, Rohn TT. Caspase-mediated cleavage of glial fibrillary acidic protein within degenerating astrocytes of the Alzheimer's disease brain. Am J Pathol. 2006; 168(3):936–46. doi: 10.2353/ajpath.2006.050798 PMID: 16507909

57. Rossi D, Brambilla L, Valori CF, Roncoroni C, Crugnola A, Yokota T, et al. Focal degeneration of astrocytes in amyotrophic lateral sclerosis. Cell Death Differ. 2008; 15(11):1691–700. doi: 10.1038/cdd.2008.99 PMID: 18617894

58. Takuma K, Baba A, Matsuda T. Astrocyte apoptosis: implications for neuroprotection. Prog Neurobiol. 2004; 72(2):111–27. doi: 10.1016/j.pneurobio.2004.02.001 PMID: 15063528

59. Liu D, Smith CL, Barone FC, Ellison JA, Lysko PG, Li K, et al. Astrocytic demise precedes delayed neuronal death in focal ischemic rat brain. Brain Res Mol Brain Res. 1999; 68(1–2):29–41. PMID: 10320781

60. Bezzi P, Domercq M, Brambilla L, Galli R, Schols D, De Clercq E, et al. CXCR4-activated astrocyte glutamate release via TNFalpha: amplification by microglia triggers neurotoxicity. Nat Neurosci. 2001; 4(7):702–10. doi: 10.1038/89490 PMID: 11426226

61. Rossi D, Brambilla L, Valori CF, Crugnola A, Giaccone G, Capobianco R, et al. Defective tumor necrosis factor-alpha-dependent control of astrocyte glutamate release in a transgenic mouse model of Alzheimer disease. J Biol Chem. 2005; 280(51):42088–96. doi: 10.1074/jbc.M504124200 PMID: 16253995

62. Foran E, Trotti D. Glutamate transporters and the excitotoxic path to motor neuron degeneration in amyotrophic lateral sclerosis. Antioxid Redox Signal. 2009; 11(7):1587–602. doi: 10.1089/ars.2009.2444 PMID: 19413484

63. Pekny M, Wilhelmsson U, Pekna M. The dual role of astrocyte activation and reactive gliosis. Neurosci Lett. 2014; 565:30–8. doi: 10.1016/j.neulet.2013.12.071 PMID: 24406153

64. Tilleux S, Hermans E. Neuroinflammation and regulation of glial glutamate uptake in neurological disorders. J Neurosci Res. 2007; 85(10):2059–70. doi: 10.1002/jnr.21325 PMID: 17497670

65. Chen Y, Swanson RA. Astrocytes and brain injury. J Cereb Blood Flow Metab. 2003; 23(2):137–49. doi: 10.1097/01.WCB.0000044631.80210.3C PMID: 12571445

66. de Lanerolle NC, Bandak F, Kang D, Li AY, Du F, Swauger P, et al. Characteristics of an explosive blast-induced brain injury in an experimental model. Journal of neuropathology and experimental

neurology. 2011; 70(11):1046–57. Epub 2011/10/18. doi: 10.1097/NEN.0b013e318235bef2 PMID: 22002430

67. Lu J, Ng KC, Ling G, Wu J, Poon DJ, Kan EM, et al. Effect of blast exposure on the brain structure and cognition in Macaca fascicularis. Journal of neurotrauma. 2012; 29(7):1434–54. Epub 2011/06/07. doi: 10.1089/neu.2010.1591 PMID: 21639720

68. Sajja VS, Galloway MP, Ghoddoussi F, Thiruthalinathan D, Kepsel A, Hay K, et al. Blast-induced neurotrauma leads to neurochemical changes and neuronal degeneration in the rat hippocampus. NMR in biomedicine. 2012; 25(12):1331–9. Epub 2012/05/03. doi: 10.1002/nbm.2805 PMID: 22549883

69. Li B, Mahmood A, Lu D, Wu H, Xiong Y, Qu C, et al. Simvastatin attenuates microglial cells and astrocyte activation and decreases interleukin-1beta level after traumatic brain injury. Neurosurgery. 2009; 65(1):179–85; discussion 85–6. Epub 2009/07/04. doi: 10.1227/01.NEU.0000346272.76537.DC PMID: 19574840

70. Sofroniew MV, Vinters HV. Astrocytes: biology and pathology. Acta Neuropathol. 2010; 119(1):7–35. doi: 10.1007/s00401-009-0619-8 PMID: 20012068

71. Conti AC, Raghupathi R, Trojanowski JQ, McIntosh TK. Experimental brain injury induces regionally distinct apoptosis during the acute and delayed post-traumatic period. J Neurosci. 1998; 18(15):5663–72. PMID: 9671657

72. Johnson EA, Svetlov SI, Wang KK, Hayes RL, Pineda JA. Cell-specific DNA fragmentation may be attenuated by a survivin-dependent mechanism after traumatic brain injury in rats. Exp Brain Res. 2005; 167(1):17–26. doi: 10.1007/s00221-005-2362-2 PMID: 16193270

73. Newcomb JK, Zhao X, Pike BR, Hayes RL. Temporal profile of apoptotic-like changes in neurons and astrocytes following controlled cortical impact injury in the rat. Exp Neurol. 1999; 158(1):76–88. doi: 10.1006/exnr.1999.7071 PMID: 10448419

74. Zhao X, Ahram A, Berman RF, Muizelaar JP, Lyeth BG. Early loss of astrocytes after experimental traumatic brain injury. Glia. 2003; 44(2):140–52. doi: 10.1002/glia.10283 PMID: 14515330

75. van Landeghem FK, Stover JF, Bechmann I, Bruck W, Unterberg A, Buhrer C, et al. Early expression of glutamate transporter proteins in ramified microglia after controlled cortical impact injury in the rat. Glia. 2001; 35(3):167–79. PMID: 11494408

76. van Landeghem FK, Weiss T, Oehmichen M, von Deimling A. Decreased expression of glutamate transporters in astrocytes after human traumatic brain injury. Journal of neurotrauma. 2006; 23 (10):1518–28. doi: 10.1089/neu.2006.23.1518 PMID: 17020486

77. Castejon OJ. Biopathology of astrocytes in human traumatic and complicated brain injuries. Review and hypothesis. Folia Neuropathol. 2015; 53(3):173–92. doi: 10.5114/fn.2015.54419 PMID: 26443309

78. Pun PB, Kan EM, Salim A, Li Z, Ng KC, Moochhala SM, et al. Low level primary blast injury in rodent brain. Frontiers in neurology. 2011; 2:19. Epub 2011/05/05. doi: 10.3389/fneur.2011.00019 PMID: 21541261

79. Mewes A, Franke H, Singer D. Organotypic brain slice cultures of adult transgenic P301S mice—a model for tauopathy studies. PloS one. 2012; 7(9):e45017. doi: 10.1371/journal.pone.0045017 PMID: 22984603

80. Coltman BW, Ide CF. Temporal characterization of microglia, IL-1 beta-like immunoreactivity and astrocytes in the dentate gyrus of hippocampal organotypic slice cultures. International journal of developmental neuroscience: the official journal of the International Society for Developmental Neuroscience. 1996; 14(6):707–19. Epub 1996/10/01.

81. Benediktsson AM, Schachtele SJ, Green SH, Dailey ME. Ballistic labeling and dynamic imaging of astrocytes in organotypic hippocampal slice cultures. Journal of neuroscience methods. 2005; 141 (1):41–53. doi: 10.1016/j.jneumeth.2004.05.013 PMID: 15585287

82. Molofsky AV, Krencik R, Ullian EM, Tsai HH, Deneen B, Richardson WD, et al. Astrocytes and disease: a neurodevelopmental perspective. Genes Dev. 2012; 26(9):891–907. doi: 10.1101/gad.188326.112 PMID: 22549954

83. Stoppini L, Buchs PA, Muller D. A simple method for organotypic cultures of nervous tissue. Journal of neuroscience methods. 1991; 37(2):173–82. Epub 1991/04/01. PMID: 1715499

84. Adamchik Y, Frantseva MV, Weisspapir M, Carlen PL, Perez Velazquez JL. Methods to induce primary and secondary traumatic damage in organotypic hippocampal slice cultures. Brain research Brain research protocols. 2000; 5(2):153–8. PMID: 10775835

85. Coburn M, Maze M, Franks NP. The neuroprotective effects of xenon and helium in an in vitro model of traumatic brain injury. Critical care medicine. 2008; 36(2):588–95. Epub 2008/01/25. doi: 10.1097/01.CCM.0B013E3181611F8A6 PMID: 18216607

86. Sarnowska A, Braun H, Sauerzweig S, Reymann KG. The neuroprotective effect of bone marrow stem cells is not dependent on direct cell contact with hypoxic injured tissue. Exp Neurol. 2009; 215 (2):317–27. Epub 2008/12/10. doi: 10.1016/j.expneurol.2008.10.023 PMID: 19063882

87. Fahlenkamp AV, Coburn M, Czaplik M, Ryang YM, Kipp M, Rossaint R, et al. Expression analysis of the early chemokine response 4 h after in vitro traumatic brain injury. Inflammation research: official journal of the European Histamine Research Society [et al]. 2011; 60(4):379–87. Epub 2010/11/26.

88. Chechneva O, Dinkel K, Schrader D, Reymann KG. Identification and characterization of two neurogenic zones in interface organotypic hippocampal slice cultures. Neuroscience. 2005; 136(1):343–55. Epub 2005/10/04. doi: 10.1016/j.neuroscience.2005.07.058 PMID: 16198493

89. Czapiga M, Colton CA. Function of microglia in organotypic slice cultures. J Neurosci Res. 1999; 56 (6):644–51. Epub 1999/06/22. doi: 10.1002/(SICI)1097-4547(19990615)56:6<644::AID-JNR10>3.0. CO;2-9 PMID: 10374819

90. Zhou S, Cui Z, Urban J. Dead cell counts during serum cultivation are underestimated by the fluorescent live/dead assay. Biotechnology journal. 2011; 6(5):513–8. doi: 10.1002/biot.201000254 PMID: 21305696

91. Pozzo Miller LD, Mahanty NK, Connor JA, Landis DM. Spontaneous pyramidal cell death in organotypic slice cultures from rat hippocampus is prevented by glutamate receptor antagonists. Neuroscience. 1994; 63(2):471–87. Epub 1994/11/01. PMID: 7891859

92. Petersen MA, Dailey ME. Diverse microglial motility behaviors during clearance of dead cells in hippocampal slices. Glia. 2004; 46(2):195–206. Epub 2004/03/26. doi: 10.1002/glia.10362 PMID: 15042586

93. Gahwiler BH, Capogna M, Debanne D, McKinney RA, Thompson SM. Organotypic slice cultures: a technique has come of age. Trends Neurosci. 1997; 20(10):471–7. Epub 1997/11/05. PMID: 9347615

94. Glavaski-Joksimovic A, Thonabulsombat C, Wendt M, Eriksson M, Palmgren B, Jonsson A, et al. Survival, migration, and differentiation of Sox1-GFP embryonic stem cells in coculture with an auditory brainstem slice preparation. Cloning and stem cells. 2008; 10(1):75–88. Epub 2008/02/05. doi: 10. 1089/clo.2007.0065 PMID: 18241123

95. Humpel C. Organotypic brain slice cultures: A review. Neuroscience. 2015; 305:86–98. doi: 10.1016/j. neuroscience.2015.07.086 PMID: 26254240

96. Glavaski-Joksimovic A, Thonabulsombat C, Wendt M, Eriksson M, Ma H, Olivius P. Morphological differentiation of tau-green fluorescent protein embryonic stem cells into neurons after co-culture with auditory brain stem slices. Neuroscience. 2009; 162(2):472–81. Epub 2009/05/05. doi: 10.1016/j. neuroscience.2009.04.070 PMID: 19410633

97. Zou J, Crews FT. Inflammasome-IL-1beta Signaling Mediates Ethanol Inhibition of Hippocampal Neurogenesis. Frontiers in neuroscience. 2012; 6:77. Epub 2012/06/05. doi: 10.3389/fnins.2012.00077 PMID: 22661925

98. Macklis JD, Madison RD. Progressive incorporation of propidium iodide in cultured mouse neurons correlates with declining electrophysiological status: a fluorescence scale of membrane integrity. Journal of neuroscience methods. 1990; 31(1):43–6. Epub 1990/01/01. PMID: 2308380

99. Cummings BS, Schnellmann RG. Measurement of cell death in mammalian cells. Curr Protoc Pharmacol. 2004; Chapter 12:Unit 12 8. doi: 10.1002/0471141755.ph1208s25 PMID: 22294120

100. Noraberg J, Kristensen BW, Zimmer J. Markers for neuronal degeneration in organotypic slice cultures. Brain research Brain research protocols. 1999; 3(3):278–90. Epub 1999/02/12. PMID: 9974143

101. Foraker JE, Oh JY, Ylostalo JH, Lee RH, Watanabe J, Prockop DJ. Cross-talk between human mesenchymal stem/progenitor cells (MSCs) and rat hippocampal slices in LPS-stimulated cocultures: the MSCs are activated to secrete prostaglandin E2. J Neurochem. 2011; 119(5):1052–63. Epub 2011/10/ 01. doi: 10.1111/j.1471-4159.2011.07511.x PMID: 21954847

102. Dan B, Yang X, Yue P, Qingwei L. [Molecular regulations of phosphatidylserine eversion in plasma membrane]. Yi Chuan. 2015; 37(2):140–7. doi: 10.16288/j.yczz.14-207 PMID: 25665640

103. Jurado-Arjona J, Goni-Oliver P, Rodriguez-Prada L, Engel T, Henshall DC, Avila J, et al. Excitotoxicity induced by kainic acid provokes glycogen synthase kinase-3 truncation in the hippocampus. Brain Res. 2015; 1611:84–92. doi: 10.1016/j.brainres.2015.03.016 PMID: 25779040

104. Morin-Brureau M, Lebrun A, Rousset MC, Fagni L, Bockaert J, de Bock F, et al. Epileptiform activity induces vascular remodeling and zonula occludens 1 downregulation in organotypic hippocampal cultures: role of VEGF signaling pathways. J Neurosci. 2011; 31(29):10677–88. doi: 10.1523/ JNEUROSCI.5692-10.2011 PMID: 21775611

105. Cimarosti H, Kantamneni S, Henley JM. Ischaemia differentially regulates GABA(B) receptor subunits in organotypic hippocampal slice cultures. Neuropharmacology. 2009; 56(8):1088–96. doi: 10.1016/j. neuropharm.2009.03.007 PMID: 19328818

106. Campbell SL, Hablitz JJ, Olsen ML. Functional changes in glutamate transporters and astrocyte biophysical properties in a rodent model of focal cortical dysplasia. Front Cell Neurosci. 2014; 8:425. doi: 10.3389/fncel.2014.00425 PMID: 25565960

107. Singleton RH, Povlishock JT. Identification and characterization of heterogeneous neuronal injury and death in regions of diffuse brain injury: evidence for multiple independent injury phenotypes. J Neurosci. 2004; 24(14):3543–53. doi: 10.1523/JNEUROSCI.5048-03.2004 PMID: 15071102

108. Farkas O, Lifshitz J, Povlishock JT. Mechanoporation induced by diffuse traumatic brain injury: an irreversible or reversible response to injury? J Neurosci. 2006; 26(12):3130–40. doi: 10.1523/JNEUROSCI.5119-05.2006 PMID: 16554464

109. Zhang Z, Zoltewicz JS, Mondello S, Newsom KJ, Yang Z, Yang B, et al. Human traumatic brain injury induces autoantibody response against glial fibrillary acidic protein and its breakdown products. PLoS One. 2014; 9(3):e92698. doi: 10.1371/journal.pone.0092698 PMID: 24667434

110. Su T, Paradiso B, Long YS, Liao WP, Simonato M. Evaluation of cell damage in organotypic hippocampal slice culture from adult mouse: a potential model system to study neuroprotection. Brain research. 2011; 1385:68–76. Epub 2011/02/10. doi: 10.1016/j.brainres.2011.01.115 PMID: 21303673

111. Cho S, Wood A, Bowlby MR. Brain slices as models for neurodegenerative disease and screening platforms to identify novel therapeutics. Current neuropharmacology. 2007; 5(1):19–33. Epub 2008/07/11. PMID: 18615151

112. Buchs PA, Stoppini L, Muller D. Structural modifications associated with synaptic development in area CA1 of rat hippocampal organotypic cultures. Brain Res Dev Brain Res. 1993; 71(1):81–91. PMID: 8432003

113. Collin C, Miyaguchi K, Segal M. Dendritic spine density and LTP induction in cultured hippocampal slices. J Neurophysiol. 1997; 77(3):1614–23. PMID: 9084624

114. Bahr BA. Long-term hippocampal slices: a model system for investigating synaptic mechanisms and pathologic processes. J Neurosci Res. 1995; 42(3):294–305. doi: 10.1002/jnr.490420303 PMID: 8583497

115. De Simoni A, Griesinger CB, Edwards FA. Development of rat CA1 neurones in acute versus organotypic slices: role of experience in synaptic morphology and activity. J Physiol. 2003; 550(Pt 1):135–47. doi: 10.1113/jphysiol.2003.039099 PMID: 12879864

116. Morrison B 3rd, Eberwine JH, Meaney DF, McIntosh TK. Traumatic injury induces differential expression of cell death genes in organotypic brain slice cultures determined by complementary DNA array hybridization. Neuroscience. 2000; 96(1):131–9. PMID: 10683418

117. Rytter A, Cronberg T, Asztely F, Nemali S, Wieloch T. Mouse hippocampal organotypic tissue cultures exposed to in vitro "ischemia" show selective and delayed CA1 damage that is aggravated by glucose. Journal of cerebral blood flow and metabolism: official journal of the International Society of Cerebral Blood Flow and Metabolism. 2003; 23(1):23–33.

118. Morrison B 3rd, Cater HL, Benham CD, Sundstrom LE. An in vitro model of traumatic brain injury utilising two-dimensional stretch of organotypic hippocampal slice cultures. Journal of neuroscience methods. 2006; 150(2):192–201. doi: 10.1016/j.jneumeth.2005.06.014 PMID: 16098599

119. Effgen GB, Ong T, Nammalwar S, Ortuno AI, Meaney DF, Bass CR, et al. Primary Blast Exposure Increases Hippocampal Vulnerability to Subsequent Exposure: Reducing Long-Term Potentiation. Journal of neurotrauma. 2016.

120. Vogel EW 3rd, Effgen GB, Patel TP, Meaney DF, Bass CR, Morrison B 3rd. Isolated Primary Blast Inhibits Long-Term Potentiation in Organotypic Hippocampal Slice Cultures. Journal of neurotrauma. 2016; 33(7):652–61. doi: 10.1089/neu.2015.4045 PMID: 26414012

121. Chen Y, Constantini S. Caveats for using shock tube in blast-induced traumatic brain injury research. Frontiers in neurology. 2013; 4:117. doi: 10.3389/fneur.2013.00117 PMID: 23986741

122. Gullotti DM, Beamer M, Panzer MB, Chen YC, Patel TP, Yu A, et al. Significant head accelerations can influence immediate neurological impairments in a murine model of blast-induced traumatic brain injury. J Biomech Eng. 2014; 136(9):091004. doi: 10.1115/1.4027873 PMID: 24950710

123. Hue CD, Cao S, Haider SF, Vo KV, Effgen GB, Vogel E 3rd, et al. Blood-brain barrier dysfunction after primary blast injury in vitro. Journal of neurotrauma. 2013; 30(19):1652–63. doi: 10.1089/neu.2012.2773 PMID: 23581482

124. Panzer MB, Matthews KA, Yu AW, Morrison B 3rd, Meaney DF, Bass CR. A Multiscale Approach to Blast Neurotrauma Modeling: Part I—Development of Novel Test Devices for in vivo and in vitro Blast Injury Models. Frontiers in neurology. 2012; 3:46. Epub 2012/04/04. doi: 10.3389/fneur.2012.00046 PMID: 22470367

125. Svetlov SI, Prima V, Glushakova O, Svetlov A, Kirk DR, Gutierrez H, et al. Neuro-glial and systemic mechanisms of pathological responses in rat models of primary blast overpressure compared to "composite" blast. Frontiers in neurology. 2012; 3:15. doi: 10.3389/fneur.2012.00015 PMID: 22403567

126. Kabu S, Jaffer H, Petro M, Dudzinski D, Stewart D, Courtney A, et al. Blast-Associated Shock Waves Result in Increased Brain Vascular Leakage and Elevated ROS Levels in a Rat Model of Traumatic Brain Injury. PloS one. 2015; 10(5):e0127971. doi: 10.1371/journal.pone.0127971 PMID: 26024446

127. Lim YW, Meyer NP, Shah AS, Budde MD, Stemper BD, Olsen CM. Voluntary Alcohol Intake following Blast Exposure in a Rat Model of Mild Traumatic Brain Injury. PloS one. 2015; 10(4):e0125130. doi: 10.1371/journal.pone.0125130 PMID: 25910266

128. Willoughby KA, Kleindienst A, Muller C, Chen T, Muir JK, Ellis EF. S100B protein is released by in vitro trauma and reduces delayed neuronal injury. J Neurochem. 2004; 91(6):1284–91. doi: 10.1111/j.1471-4159.2004.02812.x PMID: 15584905

129. Ellis EF, McKinney JS, Willoughby KA, Liang S, Povlishock JT. A new model for rapid stretch-induced injury of cells in culture: characterization of the model using astrocytes. Journal of neurotrauma. 1995; 12(3):325–39. doi: 10.1089/neu.1995.12.325 PMID: 7473807

130. Vandevord PJ, Leung LY, Hardy W, Mason M, Yang KH, King AI. Up-regulation of reactivity and survival genes in astrocytes after exposure to short duration overpressure. Neurosci Lett. 2008; 434 (3):247–52. Epub 2008/03/18. doi: 10.1016/j.neulet.2008.01.056 PMID: 18342445

131. Hlavac N, Miller S, Grinter M, VandeVord P. Two and Three-Dimensional in Vitro Models of Blast-Induced Neurotrauma. Biomed Sci Instrum. 2015; 51:439–45. PMID: 25996750

132. Sosa MA, De Gasperi R, Paulino AJ, Pricop PE, Shaughness MC, Maudlin-Jeronimo E, et al. Blast overpressure induces shear-related injuries in the brain of rats exposed to a mild traumatic brain injury. Acta neuropathologica communications. 2013; 1(1):51. Epub 2013/11/21.

133. Vandevord PJ, Bolander R, Sajja VS, Hay K, Bir CA. Mild neurotrauma indicates a range-specific pressure response to low level shock wave exposure. Annals of biomedical engineering. 2012; 40(1):227–36. Epub 2011/10/14. doi: 10.1007/s10439-011-0420-4 PMID: 21994066

134. Garman RH, Jenkins LW, Switzer RC 3rd, Bauman RA, Tong LC, Swauger PV, et al. Blast exposure in rats with body shielding is characterized primarily by diffuse axonal injury. Journal of neurotrauma. 2011; 28(6):947–59. Epub 2011/04/01. doi: 10.1089/neu.2010.1540 PMID: 21449683

135. Heldt SA, Elberger AJ, Deng Y, Guley NH, Del Mar N, Rogers J, et al. A novel closed-head model of mild traumatic brain injury caused by primary overpressure blast to the cranium produces sustained emotional deficits in mice. Frontiers in neurology. 2014; 5:2. doi: 10.3389/fneur.2014.00002 PMID: 24478749

136. Sawyer TW, Wang Y, Ritzel DV, Josey T, Villanueva M, Shei Y, et al. High-Fidelity Simulation of Primary Blast: Direct Effects on the Head. Journal of neurotrauma. 2016.

137. Suh EC, Jung YJ, Kim YA, Park EM, Lee KE. A beta 25–35 induces presynaptic changes in organotypic hippocampal slice cultures. Neurotoxicology. 2008; 29(4):691–9. Epub 2008/05/27. doi: 10.1016/j.neuro.2008.04.001 PMID: 18502514

138. Mari C, Karabiyikoglu M, Goris ML, Tait JF, Yenari MA, Blankenberg FG. Detection of focal hypoxic-ischemic injury and neuronal stress in a rodent model of unilateral MCA occlusion/reperfusion using radiolabeled annexin V. Eur J Nucl Med Mol Imaging. 2004; 31(5):733–9. doi: 10.1007/s00259-004-1473-5 PMID: 14985868

139. Wong J, Hoe NW, Zhiwei F, Ng I. Apoptosis and traumatic brain injury. Neurocrit Care. 2005; 3 (2):177–82. doi: 10.1385/NCC:3:2:177 PMID: 16174891

140. Huang Q, Zhang R, Zou L, Cao X, Chu X. Cell death pathways in astrocytes with a modified model of oxygen-glucose deprivation. PloS one. 2013; 8(4):e61345. doi: 10.1371/journal.pone.0061345 PMID: 23637816

141. Zuo H, Lin T, Wang D, Peng R, Wang S, Gao Y, et al. Neural cell apoptosis induced by microwave exposure through mitochondria-dependent caspase-3 pathway. Int J Med Sci. 2014; 11(5):426–35. doi: 10.7150/ijms.6540 PMID: 24688304

142. Chen J, Li X, Qiu J, You H, Zhang Q, Dong G, et al. Kinetics of apoptosis and expression of apoptosis-related proteins in rat CA3 hippocampus cells after experimental diffuse brain injury. Cell Biochem Biophys. 2013; 67(3):1015–9. doi: 10.1007/s12013-013-9597-5 PMID: 23559276

143. Kuehn R, Simard PF, Driscoll I, Keledjian K, Ivanova S, Tosun C, et al. Rodent model of direct cranial blast injury. Journal of neurotrauma. 2011; 28(10):2155–69. Epub 2011/06/07. doi: 10.1089/neu.2010.1532 PMID: 21639724

144. Yong-Ming Z, Jia-Chuan L, Yan-Yan Y, Wen-Jiang S, Hong T, Bing-Cang L, et al. Effective protection of rabbits' explosive brain injury through blocking gap junction communication. African health sciences. 2012; 12(4):552–6. Epub 2013/03/22. PMID: 23515469

145. Kato K, Fujimura M, Nakagawa A, Saito A, Ohki T, Takayama K, et al. Pressure-dependent effect of shock waves on rat brain: induction of neuronal apoptosis mediated by a caspase-dependent pathway. Journal of neurosurgery. 2007; 106(4):667–76. Epub 2007/04/17. doi: 10.3171/jns.2007.106.4.667 PMID: 17432720

146. Hulse RE, Winterfield J, Kunkler PE, Kraig RP. Astrocytic clasmatodendrosis in hippocampal organ culture. Glia. 2001; 33(2):169–79. PMID: 11180514

147. Zhu F, Chou CC, Yang KH, King AI. Development of a new biomechanical indicator for primary blast-induced brain injury. Chin J Traumatol. 2015; 18(1):10–2. PMID: 26169087

148. Kodama T, Uenohara H, Takayama K. Innovative technology for tissue disruption by explosive-induced shock waves. Ultrasound Med Biol. 1998; 24(9):1459–66. PMID: 10385967

149. Jayakumar AR, Tong XY, Ruiz-Cordero R, Bregy A, Bethea JR, Bramlett HM, et al. Activation of NF-kappaB mediates astrocyte swelling and brain edema in traumatic brain injury. Journal of neuro-trauma. 2014; 31(14):1249–57. doi: 10.1089/neu.2013.3169 PMID: 24471369

150. Jayakumar AR, Rao KV, Panickar KS, Moriyama M, Reddy PV, Norenberg MD. Trauma-induced cell swelling in cultured astrocytes. Journal of neuropathology and experimental neurology. 2008; 67 (5):417–27. doi: 10.1097/NEN.0b013e31816fc9d4 PMID: 18431255

151. Wang KW, Qi ST, Yang ZH, Wang ZG, Zhu PF, Yang KJ, et al. [Ultrastructural features of cultured rat cortical astrocytes with stretch-induced injury]. Di Yi Jun Yi Da Xue Xue Bao. 2002; 22(8):687–9. PMID: 12376249

152. Kaur C, Singh J, Lim MK, Ng BL, Yap EP, Ling EA. Ultrastructural changes of macroglial cells in the rat brain following an exposure to a non-penetrative blast. Annals of the Academy of Medicine, Singapore. 1997; 26(1):27–9. Epub 1997/01/01. PMID: 9140574

153. Bullock R, Maxwell WL, Graham DI, Teasdale GM, Adams JH. Glial swelling following human cerebral contusion: an ultrastructural study. J Neurol Neurosurg Psychiatry. 1991; 54(5):427–34. PMID: 1865206

154. Sakai K, Fukuda T, Iwadate K. Beading of the astrocytic processes (clasmatodendrosis) following head trauma is associated with protein degradation pathways. Brain Inj. 2013; 27(13–14):1692–7. doi: 10.3109/02699052.2013.837198 PMID: 24111565

155. Ryu HJ, Kim JE, Yeo SI, Kim DW, Kwon OS, Choi SY, et al. F-actin depolymerization accelerates clas-matodendrosis via activation of lysosome-derived autophagic astroglial death. Brain Res Bull. 2011; 85(6):368–73. doi: 10.1016/j.brainresbull.2011.05.007 PMID: 21624438

156. Ryu HJ, Kim JE, Yeo SI, Kang TC. p65/RelA-Ser529 NF-kappaB subunit phosphorylation induces autophagic astroglial death (Clasmatodendrosis) following status epilepticus. Cell Mol Neurobiol. 2011; 31(7):1071–8. doi: 10.1007/s10571-011-9706-1 PMID: 21598036

157. Clark RS, Bayir H, Chu CT, Alber SM, Kochanek PM, Watkins SC. Autophagy is increased in mice after traumatic brain injury and is detectable in human brain after trauma and critical illness. Autop-hagy. 2008; 4(1):88–90. PMID: 17957135

158. Diskin T, Tal-Or P, Erlich S, Mizrachy L, Alexandrovich A, Shohami E, et al. Closed head injury induces upregulation of Beclin 1 at the cortical site of injury. Journal of neurotrauma. 2005; 22(7):750–62. doi: 10.1089/neu.2005.22.750 PMID: 16004578

159. Sadasivan S, Dunn WA Jr., Hayes RL, Wang KK. Changes in autophagy proteins in a rat model of con-trolled cortical impact induced brain injury. Biochem Biophys Res Commun. 2008; 373(4):478–81. doi: 10.1016/j.bbrc.2008.05.031 PMID: 18486600

160. Luo CL, Li BX, Li QQ, Chen XP, Sun YX, Bao HJ, et al. Autophagy is involved in traumatic brain injury-induced cell death and contributes to functional outcome deficits in mice. Neuroscience. 2011; 184:54–63. doi: 10.1016/j.neuroscience.2011.03.021 PMID: 21463664

161. Liu J, Liu MC, Wang KK. Calpain in the CNS: from synaptic function to neurotoxicity. Sci Signal. 2008; 1(14):re1. doi: 10.1126/stke.114re1 PMID: 18398107

162. Saatman KE, Creed J, Raghupathi R. Calpain as a therapeutic target in traumatic brain injury. Neu-rotherapeutics. 2010; 7(1):31–42. doi: 10.1016/j.nurt.2009.11.002 PMID: 20129495

163. Bralic M, Stemberga V, Stifter S. Introduction of calpain inhibitors in traumatic brain injury: a novel approach? Medical hypotheses. 2012; 79(3):358–60. doi: 10.1016/j.mehy.2012.05.034 PMID: 22726623

164. Liu MC, Akle V, Zheng W, Dave JR, Tortella FC, Hayes RL, et al. Comparing calpain- and caspase-3-mediated degradation patterns in traumatic brain injury by differential proteome analysis. Biochem J. 2006; 394(Pt 3):715–25. doi: 10.1042/BJ20050905 PMID: 16351572

165. Valiyaveettil M, Alamneh YA, Wang Y, Arun P, Oguntayo S, Wei Y, et al. Cytoskeletal protein alpha-II spectrin degradation in the brain of repeated blast exposed mice. Brain Res. 2014; 1549:32–41. doi: 10.1016/j.brainres.2013.12.031 PMID: 24412202

166. Yang Z, Lin F, Robertson CS, Wang KK. Dual vulnerability of TDP-43 to calpain and caspase-3 proteolysis after neurotoxic conditions and traumatic brain injury. Journal of cerebral blood flow and metabolism: official journal of the International Society of Cerebral Blood Flow and Metabolism. 2014; 34 (9):1444–52.

167. Lee YB, Du S, Rhim H, Lee EB, Markelonis GJ, Oh TH. Rapid increase in immunoreactivity to GFAP in astrocytes in vitro induced by acidic pH is mediated by calcium influx and calpain I. Brain research. 2000; 864(2):220–9. PMID: 10802029

168. Lumpkins KM, Bochicchio GV, Keledjian K, Simard JM, McCunn M, Scalea T. Glial fibrillary acidic protein is highly correlated with brain injury. The Journal of trauma. 2008; 65(4):778–82; discussion 82–4. doi: 10.1097/TA.0b013e318185db2d PMID: 18849790

169. Lee JY, Lee CY, Kim HR, Lee CH, Kim HW, Kim JH. A Role of Serum-Based Neuronal and Glial Markers as Potential Predictors for Distinguishing Severity and Related Outcomes in Traumatic Brain Injury. J Korean Neurosurg Soc. 2015; 58(2):93–100. doi: 10.3340/jkns.2015.58.2.93 PMID: 26361523

170. Lei J, Gao G, Feng J, Jin Y, Wang C, Mao Q, et al. Glial fibrillary acidic protein as a biomarker in severe traumatic brain injury patients: a prospective cohort study. Crit Care. 2015; 19:362. doi: 10.1186/s13054-015-1081-8 PMID: 26455520

171. Papa L, Lewis LM, Falk JL, Zhang Z, Silvestri S, Giordano P, et al. Elevated levels of serum glial fibrillary acidic protein breakdown products in mild and moderate traumatic brain injury are associated with intracranial lesions and neurosurgical intervention. Ann Emerg Med. 2012; 59(6):471–83. doi: 10.1016/j.annemergmed.2011.08.021 PMID: 22071014

172. Okonkwo DO, Yue JK, Puccio AM, Panczykowski DM, Inoue T, McMahon PJ, et al. GFAP-BDP as an acute diagnostic marker in traumatic brain injury: results from the prospective transforming research and clinical knowledge in traumatic brain injury study. Journal of neurotrauma. 2013; 30(17):1490–7. doi: 10.1089/neu.2013.2883 PMID: 23489259

173. Yang Z, Wang KK. Glial fibrillary acidic protein: from intermediate filament assembly and gliosis to neurobiomarker. Trends Neurosci. 2015; 38(6):364–74. doi: 10.1016/j.tins.2015.04.003 PMID: 25975510

174. Levine J, Kwon E, Paez P, Yan W, Czerwieniec G, Loo JA, et al. Traumatically injured astrocytes release a proteomic signature modulated by STAT3-dependent cell survival. Glia. 2015.

175. Ralay Ranaivo H, Zunich SM, Choi N, Hodge JN, Wainwright MS. Mild stretch-induced injury increases susceptibility to interleukin-1beta-induced release of matrix metalloproteinase-9 from astrocytes. Journal of neurotrauma. 2011; 28(9):1757–66. doi: 10.1089/neu.2011.1799 PMID: 21732764

176. Whalen MJ, Dalkara T, You Z, Qiu J, Bermpohl D, Mehta N, et al. Acute plasmalemma permeability and protracted clearance of injured cells after controlled cortical impact in mice. Journal of cerebral blood flow and metabolism: official journal of the International Society of Cerebral Blood Flow and Metabolism. 2008; 28(3):490–505.

177. Pettus EH, Christman CW, Giebel ML, Povlishock JT. Traumatically induced altered membrane permeability: its relationship to traumatically induced reactive axonal change. Journal of neurotrauma. 1994; 11(5):507–22. doi: 10.1089/neu.1994.11.507 PMID: 7861444

178. Suneson A, Hansson HA, Lycke E, Seeman T. Pressure wave injuries to rat dorsal root ganglion cells in culture caused by high-energy missiles. The Journal of trauma. 1989; 29(1):10–8. Epub 1989/01/01. PMID: 2911086

179. Arun P, Abu-Taleb R, Oguntayo S, Tanaka M, Wang Y, Valiyaveettil M, et al. Distinct patterns of expression of traumatic brain injury biomarkers after blast exposure: role of compromised cell membrane integrity. Neurosci Lett. 2013; 552:87–91. Epub 2013/08/13. doi: 10.1016/j.neulet.2013.07.047 PMID: 23933206

180. Zimmer J, Kristensen BW, Jakobsen B, Noraberg J. Excitatory amino acid neurotoxicity and modulation of glutamate receptor expression in organotypic brain slice cultures. Amino Acids. 2000; 19(1):7–21. PMID: 11026469

181. Krishnamurthy K, Laskowitz DT. Cellular and Molecular Mechanisms of Secondary Neuronal Injury following Traumatic Brain Injury. In: Laskowitz D, Grant G, editors. Translational Research in Traumatic Brain Injury. Frontiers in Neuroscience. Boca Raton (FL)2016.

182. Faden AI, Demediuk P, Panter SS, Vink R. The role of excitatory amino acids and NMDA receptors in traumatic brain injury. Science. 1989; 244(4906):798–800. PMID: 2567056

183. Matute C, Alberdi E, Ibarretxe G, Sanchez-Gomez MV. Excitotoxicity in glial cells. Eur J Pharmacol. 2002; 447(2–3):239–46. PMID: 12151015

184. Rothstein JD, Dykes-Hoberg M, Pardo CA, Bristol LA, Jin L, Kuncl RW, et al. Knockout of glutamate transporters reveals a major role for astroglial transport in excitotoxicity and clearance of glutamate. Neuron. 1996; 16(3):675–86. PMID: 8785064

185. Danbolt NC. Glutamate uptake. Prog Neurobiol. 2001; 65(1):1–105. PMID: 11369436

186. Rothstein JD, Martin L, Levey AI, Dykes-Hoberg M, Jin L, Wu D, et al. Localization of neuronal and glial glutamate transporters. Neuron. 1994; 13(3):713–25. PMID: 7917301

187. Benediktsson AM, Marrs GS, Tu JC, Worley PF, Rothstein JD, Bergles DE, et al. Neuronal activity regulates glutamate transporter dynamics in developing astrocytes. Glia. 2012; 60(2):175–88. doi: 10.1002/glia.21249 PMID: 22052455

188. Furness DN, Dehnes Y, Akhtar AQ, Rossi DJ, Hamann M, Grutle NJ, et al. A quantitative assessment of glutamate uptake into hippocampal synaptic terminals and astrocytes: new insights into a neuronal role for excitatory amino acid transporter 2 (EAAT2). Neuroscience. 2008; 157(1):80–94. doi: 10.1016/j.neuroscience.2008.08.043 PMID: 18805467

189. Mennerick S, Dhond RP, Benz A, Xu W, Rothstein JD, Danbolt NC, et al. Neuronal expression of the glutamate transporter GLT-1 in hippocampal microcultures. J Neurosci. 1998; 18(12):4490–9. PMID: 9614226

190. Palmer AM, Marion DW, Botscheller ML, Swedlow PE, Styren SD, DeKosky ST. Traumatic brain injury-induced excitotoxicity assessed in a controlled cortical impact model. J Neurochem. 1993; 61(6):2015–24. PMID: 7504079

191. Yi JH, Hazell AS. Excitotoxic mechanisms and the role of astrocytic glutamate transporters in traumatic brain injury. Neurochem Int. 2006; 48(5):394–403. doi: 10.1016/j.neuint.2005.12.001 PMID: 16473439

192. Rao VL, Baskaya MK, Dogan A, Rothstein JD, Dempsey RJ. Traumatic brain injury down-regulates glial glutamate transporter (GLT-1 and GLAST) proteins in rat brain. J Neurochem. 1998; 70(5):2020–7. PMID: 9572288

193. Yi JH, Pow DV, Hazell AS. Early loss of the glutamate transporter splice-variant GLT-1v in rat cerebral cortex following lateral fluid-percussion injury. Glia. 2005; 49(1):121–33. doi: 10.1002/glia.20099 PMID: 15390098